J|A|C|S
ARTICLES
Published on Web 04/17/2002

Second Generation Light-Driven Molecular Motors. Unidirectional Rotation Controlled by a Single Stereogenic Center with Near-Perfect Photoequilibria and Acceleration of the Speed of Rotation by Structural Modification

Nagatoshi Koumura, Edzard M. Geertsema, Marc B. van Gelder, Auke Meetsma, and Ben L. Feringa*

Contribution from the Department of Organic and Molecular Inorganic Chemistry, Stratingh Institute, University of Groningen, Nijenborgh 4, 9747 AG Groningen, The Netherlands

Received November 7, 2001

Abstract: Nine new molecular motors, consisting of a 2,3-dihydro-2-methylnaphtho[2,1-*b*]thiopyran or 2,3-dihydro-3-methylphenanthrene upper part and a (thio)xanthene, 10,10-dimethylanthracene, or dibenzocycloheptene lower part, connected by a central double bond, were synthesized. A single stereogenic center, bearing a methyl substituent, is present in each of the motors. MOPAC93-AM1 calculations, NMR studies, and X-ray analysis revealed that these compounds have stable isomers with pseudoaxial orientation of the methyl substituent and less-stable isomers with pseudoequatorial orientation of the methyl substituent. The photochemical and thermal isomerization processes of the motors were studied by NMR and CD spectroscopy. The new molecular motors all show two cis−trans isomerizations upon irradiation, each followed by a thermal helix inversion, resulting in a 360° rotation around the central double bond of the upper part with respect to the lower part. The direction of rotation is controlled by a single stereogenic center created by the methyl substituent at the upper part. The speed of rotation, governed by the two thermal steps, was adjusted to a great extent by structural modifications, with half-lives for the thermal isomerization steps ranging from $t_{1/2}^{\theta}$ 233−0.67 h. The photochemical conversions of two new motors proceeded with near-perfect photoequilibria of 1:99.

Introduction

Molecular motors such as the ATP-synthase rotary motor[1] and the muscle linear motor[2] are among the most fascinating systems found in nature. The dynamic biological processes involved are reminiscent of the movement in artificial motors, ubiquitous in macroscopic machinery common to daily life, in which energy consumption is utilized to accomplish controlled motion.[3] In the recent endeavor toward nanotechnology and molecular machinery, the biological motors are a main source of inspiration.[4] Attempts to mimic the dynamic behavior via synthetic design have resulted in several elegant molecular systems in which translational or rotary motion is controlled by means of chemical, electrochemical, photochemical, or thermal input. Prominent examples are molecular ratchets,[5] turnstiles,[6] rotors,[7] and a variety of molecular switches.[8] Catenanes and rotaxanes comprise a family of compounds which have shown to be particularly useful to demonstrate several features essential to molecular machines[8b,9] like translational motion of a ring on a string in a rotaxane[10] or circumrotation of two rings in a catenane.[10a,11] Sauvage and co-workers reported the contraction and stretching of a linear rotaxane dimer resembling a natural muscle at work.[12] Recently, Stoddart and Zink demonstrated the threading and dethreading of rotaxanes assembled on a surface.[13] Rotation in metal bisporphyrinate double decker complexes in response to external electrochemical stimuli was accomplished by Aida and co-workers.[12b,14]

* To whom correspondence should be addressed. E-mail: b.l.feringa@chem.rug.nl.

(1) (a) Boyer, P. D. *Biochim. Biophys. Acta* **1993**, *1140*, 215−250. (b) Abrahams, J. P.; Leslie, A. G. W.; Lutter, R.; Walker, J. E. *Nature* **1994**, *370*, 621−628. (c) Noji, H.; Yasuda, R.; Yoshida, M.; Kinosita, K., Jr. *Nature* **1997**, *386*, 299−302. (d) Mehta, A. D.; Rief, M.; Spudich, J. A.; Smith, D. A.; Simmons, R. M. *Science* **1999**, *283*, 1689−1695. (e) Sambongi, Y.; Iko, Y.; Tanabe, M.; Omote, H.; Iwamoto-Kihara, A.; Ueda, I.; Yanagida, T.; Wada, Y.; Futai, M. *Science* **1999**, *286*, 1722−1724.

(2) (a) Finer, J. T.; Simmons, R. M.; Spudich, J. A. *Nature* **1994**, *368*, 113−119. (b) Kitamura, K.; Tokunaga, M.; Iwane, A. H.; Yanagida, T. *Nature* **1999**, *397*, 129−134. (c) Veigel, C.; Coluccio, L. M.; Jontes, J. D.; Sparrow, J. C.; Milligan, R. A.; Molloy, J. E. *Nature* **1999**, *398*, 530−533. (d) Wells, A. L.; Lin, A. W.; Chen, L.-Q.; Safer, D.; Cain, S. M.; Hasson, T.; Carragher, B. O.; Milligan, R. A.; Sweeney, H. L. *Nature* **1999**, *401*, 505−508. (e) Walker, M. L.; Burgess, S. A.; Sellars, J. R.; Waang, F.; Hammler, J. A., III; Trinick, J.; Knight, P. J. *Nature* **2000**, *405*, 804−807. (f) Endow, S. A.; Higuchi, H. *Nature* **2000**, *406*, 913−916.

(3) Special issue of *Science* **2000**, *288*, 79−106; Movement: molecular to robotic.

(4) Feringa, B. L. *Acc. Chem. Res.* **2001**, *34*, 504−513.

(5) Kelly, T. R.; Tellitu, I.; Sestelo, J. P. *Angew. Chem., Int. Ed. Engl.* **1997**, *36*, 1866−1868.

(6) Bedard, T. C.; Moore, J. S. *J. Am. Chem. Soc.* **1995**, *117*, 10662−10671.

(7) (a) Mislow, K. *Chemtracts: Org. Chem.* **1989**, *2*, 151−174. (b) Schoevaars, A. M.; Kruizinga, W.; Zijlstra, R. W. J.; Veldman, N.; Spek, A. L.; Feringa, B. L. *J. Org. Chem.* **1997**, *62*, 4943−4948.

(8) (a) Feringa, B. L.; van Delden, R. A.; Koumura, N.; Geertsema, E. M. *Chem. Rev.* **2000**, *100*, 1789−1816. (b) Feringa, B. L., Ed. *Molecular Switches*; Wiley-VCH: Weinheim, 2001.

(9) (a) Balzani, V.; Credi, A.; Raymo, F. M.; Stoddart, J. F. *Angew. Chem., Int. Ed.* **2000**, *39*, 3348−3391. (b) Sauvage, J.-P., Amendola, V., Eds. *Molecular Machines and Motors*; Springer: Berlin, 2001. (c) Special issue on Molecular Machines: *Acc. Chem. Res.* **2001**, *34*, 409−522.

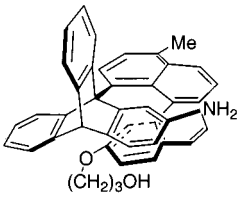

Triptycene derivative by Kelly[15]

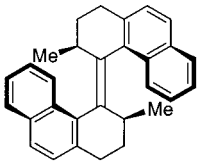

Biphenanthrylidenes by Harada and Feringa[16]
(First Light-Driven Molecular Motor)

Figure 1. The structures of the first synthetic molecular motors showing unidirectional rotation.

The following basic requirements must be satisfied in any successful design of a rotary molecular motor: (i) rotary motion, (ii) energy consumption, and (iii) unidirectional rotation.

The first synthetic molecular motors, performing unidirectional rotary motion upon energy uptake, were reported simultaneously by Kelly[15] (Figure 1a) and Harada and Feringa[16] (Figure 1b) in 1999. In both systems, molecular chirality turned out to be an essential feature to induce unidirectional rotation.

Kelly's motor comprises a helicene connected to a triptycene unit which undergo a 120° rotation with respect to each other exclusively in one direction induced by a number of chemical steps.[15] The architecture of the Harada−Feringa light-driven molecular motor is based on helical-shaped sterically overcrowded alkenes (symmetric biphenanthrylidenes).[16] Repetitive unidirectional rotation around the central double bond is achieved by two photochemical trans−cis isomerizations, each followed by a thermal conversion which adds up to a four-step cycle completing a full 360° rotation process. It was established that the direction of rotation − clockwise or counterclockwise − is governed by the two stereogenic centers present in the molecule. Further important structural features in this first generation light-driven molecular motor are the identical nature of the upper and lower parts of the tetrahydrobiphenanthrylidene and the all-carbon framework of the molecule. In the second generation molecular motors, we introduced distinct upper and lower halves as well as heteroatoms that allow tuning of the rotary motion. The synthesis and dynamic properties of the second generation molecular motors are reported here.[17]

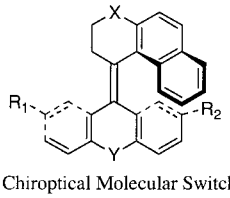

Chiroptical Molecular Switches

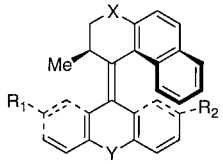

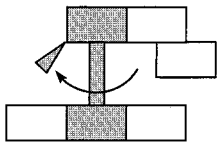

Second Generation Light-Driven Molecular Motors

Figure 2. General structures of chiroptical molecular switches and schematic view and structures of second generation molecular motors.

Molecular Design

The successful demonstration of unidirectional rotary motion with a light-driven molecular motor immediately raised the question if these systems would be suitable to be connected to surfaces or become part of multicomponent systems as ultimately this will be required to be able to build molecular machinery. For such a purpose, extensive modification and functionalization will be necessary, and the symmetric nature of the biphenanthrylidene type motors (Figure 1b) is considered a serious drawback in such an endeavor. The redesign of the molecular motors was therefore focused on systems with distinct upper and lower parts connected by a central olefinic bond that functions as the axis, as shown in Figure 2.

The molecular structure shows resemblance to the chiroptical molecular switches developed in our laboratories, and the photochemically and thermally induced dynamic processes of several members of these switches have been examined.[8,18] By introducing a methyl substituent at the upper half, a stereogenic center is present besides the helical shape of the entire molecular structure. While helix inversion (P ↔ M) can occur upon heating or irradiation (vide infra), the configuration at the stereogenic center is fixed, and this combination of stereochemical properties proved to be again crucial (as was the case with the first generation molecular motor) for unidirectional rotary motion.

The symmetric lower half of the second generation molecular motors (Figure 2) can be used for further functionalization, for instance, for ultimate connection of the motor to a surface, whereas the upper half still acts as a propeller.

Another challenge we envision that has to be addressed is the acceleration of the rotary motion by lowering the thermal isomerization barriers for helix inversion. It should be noted that in the first generation molecular motors (Figure 1), the thermal, helix inversion steps govern the rotation rate during

(10) (a) Sauvage, J.-P., Dietrich-Buchecker, C. O., Eds. *Molecular Catenanes, Rotaxanes, and Knots*; Wiley-VCH: Weinheim, 1999. (b) Bissell, R. A.; Córdova, E.; Kaifer, A. E.; Stoddart, J. F. *Nature* **1994**, *369*, 133−137. (c) Collin, J.-P.; Gaviña, P.; Sauvage, J.-P. *New J. Chem.* **1997**, *21*, 525−528. (d) Murakami, H.; Kawabuchi, A.; Kotoo, K.; Kunitaka, M.; Nakashima, N. *J. Am. Chem. Soc.* **1997**, *119*, 7605−7606. (e) Lane, A. S.; Leigh, D. A.; Murphy, A. *J. Am. Chem. Soc.* **1997**, *119*, 11092−11093. (f) Armaroli, N.; Balzani, V.; Collin, J.-P.; Gaviña, P.; Sauvage, J.-P.; Ventura, B. *J. Am. Chem. Soc.* **1999**, *121*, 4397−4408. (g) Ashton, P. R.; Ballardini, R.; Balzani, V.; Credi, A.; Dress, K. R.; Ishow, E.; Kleverlaan, C. J.; Kocian, O.; Preece, J. A.; Spencer, N.; Stoddart, J. F.; Venturi, M.; Wenger, S. *Chem.-Eur. J.* **2000**, *6*, 3558−3574. (h) Brouwer, A. M.; Frochot, C.; Gatti, F. G.; Leigh, D. A.; Mottier, L.; Paolucci, F.; Roffia, S.; Wurpel, G. W. H. *Science* **2001**, *291*, 2124−2128.

(11) (a) Ashton, P. R.; Goodnow, T. T.; Kaifer, A. E.; Reddington, M. V.; Slawin, A. M. Z.; Spencer, N.; Stoddart, J. F.; Vicent, C.; Williams, D. J. *Angew. Chem., Int. Ed. Engl.* **1989**, *28*, 1396−1399. (b) Ashton, P. R.; Pérez-García, L.; Stoddart, J. F.; White, A. J. P.; Williams, D. J. *Angew. Chem., Int. Ed. Engl.* **1995**, *34*, 571−574. (c) Balzani, V.; Credi, A.; Mattersteig, G.; Matthews, O. A.; Raymo, F. M.; Stoddart, J. F.; Venturi, M.; White, A. J. P.; Williams, D. J. *J. Org. Chem.* **2000**, *65*, 1924−1936. (d) Balzani, V.; Credi, A.; Langford, S. J.; Raymo, F. M.; Stoddart, J. F.; Venturi, M. *J. Am. Chem. Soc.* **2000**, *122*, 3542−3543.

(12) (a) Jiménez, M. C.; Dietrich-Buchecker, C.; Sauvage, J.-P. *Angew. Chem., Int. Ed.* **2000**, *39*, 3284−3287. (b) Feringa, B. L. *Nature* **2000**, *408*, 151−154; news and views, "In control of molecular motion".

(13) Chia, S.; Cao, J.; Stoddart, J. F.; Zink, J. I. *Angew. Chem., Int. Ed.* **2001**, *40*, 2447−2451.

(14) Tashiro, K.; Konishi, K.; Aida, T. *J. Am. Chem. Soc*. **2000**, *122*, 7921−7926.

(15) (a) Kelly, T. R.; De Silva, H.; Silva, R. A. *Nature* **1999**, *401*, 150−152. (b) Kelly, T. R.; Silva, R. A.; De Silva, H.; Jasmin, S.; Zhao, Y. *J. Am. Chem. Soc*. **2000**, *122*, 6935−6949.

(16) Koumura, N.; Zijlstra, R. W. J.; van Delden, R. A.; Harada, N.; Feringa, B. L. *Nature* **1999**, *401*, 152−155. See also: Davis, A. P. *Nature* **1999**, *401*, 120−121; news and views, "Synthetic Molecular Motors".

(17) Koumura, N.; Geertsema, E. M.; Meetsma, A.; Feringa, B. L. *J. Am. Chem. Soc.* **2000**, *122*, 12005−12006.

(18) (a) Feringa, B. L.; Jager, W. F.; de Lange, B.; Meÿer, E. W. *J. Am. Chem. Soc.* **1991**, *113*, 5468−5470. (b) Jager, W. F.; de Jong, J. C.; de Lange, B.; Huck, N. P. M.; Meetsma, A.; Feringa, B. L. *Angew. Chem., Int. Ed. Engl.* **1995**, *34*, 348−350. (c) Feringa, B. L.; Huck, N. P. M.; van Doren, H. A. *J. Am. Chem. Soc.* **1995**, *117*, 9929−9930.

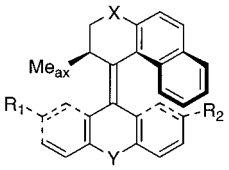

stable forms

(2′*R*)-(*M*)-*trans*-**1a**: X=S, Y=S, R_1=OMe, R_2=H
(2′*R*)-(*M*)-*cis*-**2a**: X=S, Y=S, R_1=H, R_2=OMe
(2′*R*)-(*M*)-**3a**: X=S, Y=S, R_1=H, R_2=H
(2′*R*)-(*M*)-**4a**: X=S, Y=S, R_1=OMe, R_2=OMe
(2′*R*)-(*M*)-**5a**: X=S, Y=O, R_1=H, R_2=H
(2′*R*)-(*M*)-**6a**: X=S, Y=C$(CH_3)_2$, R_1=H, R_2=H
(2′*S*)-(*M*)-**7a**: X=CH_2, Y=S, R_1=H, R_2=H
(2′*S*)-(*M*)-**8a**: X=CH_2, Y=C$(CH_3)_2$, R_1=H, R_2=H
(2′*S*)-(*M*)-**9a**: X=CH_2, Y=CHCH, R_1=H, R_2=H

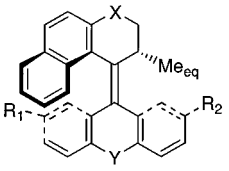

less-stable forms

(2′*R*)-(*P*)-*trans*-**1b**: X=S, Y=S, R_1=H, R_2=OMe
(2′*R*)-(*P*)-*cis*-**2b**: X=S, Y=S, R_1=OMe, R_2=H
(2′*R*)-(*P*)-**3b**: X=S, Y=S, R_1=H, R_2=H
(2′*R*)-(*P*)-**4b**: X=S, Y=S, R_1=OMe, R_2=OMe
(2′*R*)-(*P*)-**5b**: X=S, Y=O, R_1=H, R_2=H
(2′*R*)-(*P*)-**6b**: X=S, Y=C$(CH_3)_2$, R_1=H, R_2=H
(2′*S*)-(*P*)-**7b**: X=CH_2, Y=S, R_1=H, R_2=H
(2′*S*)-(*P*)-**8b**: X=CH_2, Y=C$(CH_3)_2$, R_1=H, R_2=H
(2′*S*)-(*P*)-**9b**: X=CH_2, Y=CHCH, R_1=H, R_2=H

Figure 3. The nine second generation molecular motors.

the overall 360° rotation of the two halves of the molecule with respect to each other. To be able to tune the energy barriers for the thermal steps, the bridging (hetero)atoms X and Y are systematically changed. We have previously shown that the barriers for thermal isomerization processes in symmetrically overcrowded alkenes can be effected by bridging heteroatoms.[19] The unique combination of axial chirality and a stereogenic center, the presence of both *cis*- and *trans*-stilbene type chromophores in the same structure, and distinct upper and lower halves are the most notable features of the motor design shown in Figures 2 and 3.

Results and Discussion

Conformational Aspects by Molecular Modeling Studies. As mentioned above, we expected that the helical shape of the second generation molecular motor could be controlled by the stereogenic center at the 2′-position as was shown for the first generation molecular motor, and it would be possible that two conformers of both *trans*- and *cis*-isomers **1** and **2** (Figure 3) exist. To examine this prediction and obtain information on ground-state energies of the two possible conformers, we carried out calculations on *trans*-**1** and *cis*-**2** using the MOPAC93 AM1 program.[20] As shown in Figures 4 and 5, both in the case of *trans*-**1** and *cis*-**2**, the methyl substituent at the upper part of the stable conformers (**1a** and **2a**) adopts a pseudoaxial orientation to prevent severe steric hindrance with the lower part. The other conformers (**1b** and **2b**), having a methyl group

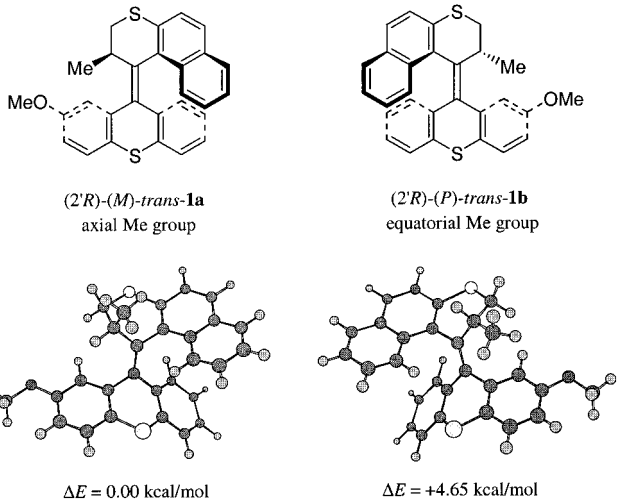

Figure 4. Molecular structures and conformations of stable (2′*R*)-(*M*)-*trans*-**1a** and less-stable (2′*R*)-(*P*)-*trans*-**1b**.

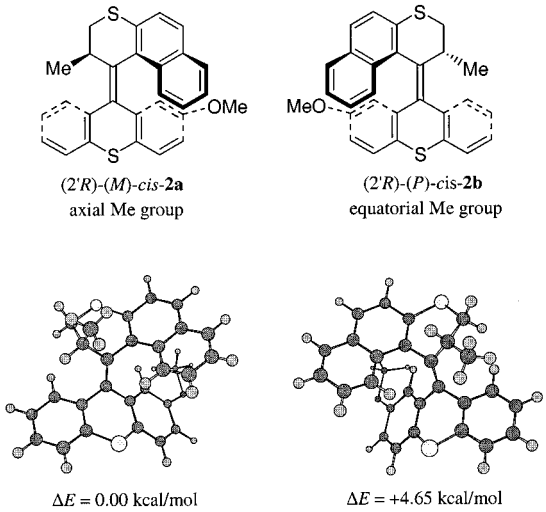

Figure 5. Molecular structures and conformations of stable (2′*R*)-(*M*)-*cis*-**2a** and less-stable (2′*R*)-(*P*)-*cis*-**2b**.

at the upper part in a pseudoequatorial orientation, are less stable. The energy differences ΔE between the stable and less-stable conformers of both *trans*-**1** and *cis*-**2** are +4.65 kcal/mol; therefore, the population of the less-stable isomer is negligible in both cases. On the basis of the results of these calculations, it appears that the helical shape of the second generation molecular motors can be controlled by the stereogenic center at the upper part and that conversion in the thermal steps from the less-stable to the stable isomers might be expected.

Synthesis of Second Generation Molecular Motors (*trans*-1a and *cis*-2a). The first version of the new type of molecular motor contains a chiral 2,3-dihydro-2-methylnaphtho[2,1-*b*]-thiopyran upper part and 2-methoxy-9-thioxanthene lower part (Figures 4 and 5). The synthesis of 2,3-dihydro-2-methyl-1*H*-naphtho[2,1-*b*]thiopyran-1-one hydrazine **13**, a precursor for the upper part of **1a** and **2a**, is shown in Scheme 1. Michael addition of 2-thionaphthol **10** to methacrylonitrile by refluxing both materials in the presence of benzyltrimethylammonium hydroxide (Triton B) provided **11**, which was converted to the cyclic ketone **12** in good yield by treatment with polyphosphoric acid. Hydrazone **13** was prepared in 60% yield from **12** in ethanol using a large excess of hydrazine monohydrate. 2-Methoxy-

(19) Feringa, B. L.; Jager, W. F.; de Lange, B. *Tetrahedron Lett.* **1992**, *33*, 2887−2890.
(20) Stewart, J. J. P. MOPAC93-AM1; Fujitsu Limited: Tokyo, Japan, 1993.

Scheme 1[a]

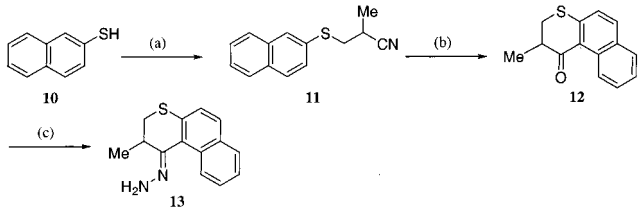

[a] (a) Triton B, methacrylonitrile, 0 → 65 °C, 85%; (b) polyphosphoric acid, 110 °C, 93%; (c) $H_2NNH_2 \cdot H_2O$/EtOH, reflux, 60%.

Scheme 2[a]

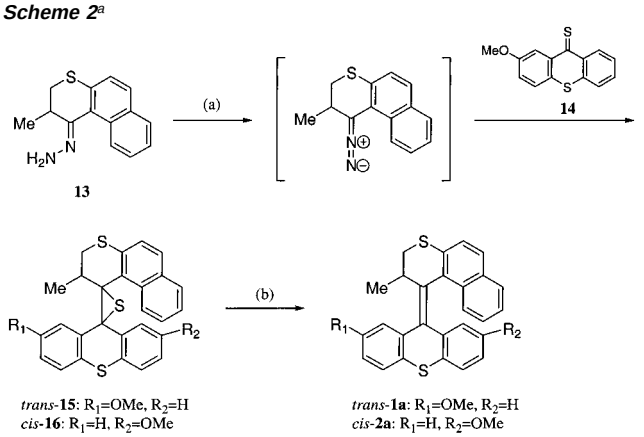

[a] (a) Ag_2O, $MgSO_4$, KOH (sat sol)/MeOH/CH_2Cl_2, 0 °C, 60%; (b) Cu-bronze/*p*-xylene, reflux, 91%.

9*H*-thioxanthene-9-thione **14**,[21,22] as a precursor of the lower part, was prepared by refluxing 2-methoxy-9*H*-thioxanthene-9-one with an excess of phosphorus pentasulfide in toluene.

The diazo-thioketone coupling reaction[23] proved to be a successful method to connect the upper and lower part of motors **1a** and **2a**.[24] In the diazo-thioketone coupling method, strain is gradually introduced via 1,3-dipolar cycloaddition to form a five-membered thiadiazolidine followed by nitrogen extrusion to three-membered episulfide and finally sulfur elimination to provide the hindered olefin. As shown in Scheme 2, hydrazone **13** was oxidized to the unstable, deep red, diazo compound with silver(I) oxide (2 equiv) in dichloromethane at −5 to 0 °C, and subsequent addition of thioketone **14** gave a mixture of *trans*- and *cis*-episulfides **15** and **16** as solids (trans/cis ratio of 1:1, 60% yield). Because separation of *trans*-**15** and *cis*-**16** could not be accomplished by flash chromatography, the mixture of *trans*-**15** and *cis*-**16** was used in the subsequent desulfurization reaction by refluxing in *p*-xylene in the presence of copper bronze to provide a mixture of *trans*- and *cis*-olefins **1a** and **2a**. These isomers could be separated by HPLC (silica gel, hexane:EtOAc = 50:1) to yield pure *trans*-**1a** (47%) and *cis*-**2a** (44%), which were fully characterized by ^{1}H, ^{13}C NMR, and HRMS. The ^{1}H NMR spectra of both isomers indicate that the absorptions of the methyl substituents at the 2′-position are shifted upfield to 0.78 ppm (*trans*-**1a**) and 0.79 ppm (*cis*-**2a**), respectively, due to aromatic ring current anisotropy. The proton absorptions of both isomers at the 2′-position are shifted downfield to 4.17 ppm (*trans*-**1a**) and 4.11 ppm (*cis*-**2a**), respectively. The unequivocal assignment of the trans- and cis-geometry was possible due to the remarkable differences between their ^{1}H NMR spectra. The absorption of the methoxy substituent at the lower part is shifted from 3.86 ppm (*trans*-**1a**) to 3.01 ppm (*cis*-**2a**) due to a shielding effect by the naphthalene moiety of the upper part in *cis*-**2a** (Table 1). To determine the relative configuration at 2′-position, ^{1}H NMR spectra of both trans- and cis-isomers were studied in detail. Coupling constants of H(2′) and H(3′) of 7.3 and 2.9 Hz (*trans*-**1a**) and 7.3 and 3.3 Hz (*cis*-**2a**) were found (Table 1), proving that the methyl groups at the 2′-position of both isomers adopt a pseudoaxial orientation.

Table 1. Selected ^{1}H NMR Data of *trans*-**1a**, *trans*-**1b**, *cis*-**2a**, and *cis*-**2b** in $CDCl_3$

compound	chemical shifts (ppm) MeO	Me	proton, H(2′)	coupling constants $J_{H(2')-H(3')}$ (Hz)
trans-**1a**	3.86	0.78	4.17	7.3, 2.9
trans-**1b**	3.85	1.17	2.74	12.1, 7.3
cis-**2a**	3.01	0.79	4.11	7.3, 3.3
cis-**2b**	2.99	1.10	2.76	12.4, 7.3

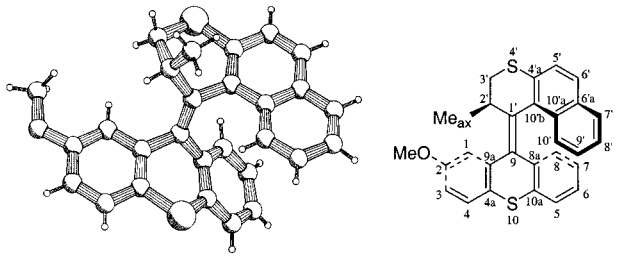

Figure 6. PLUTO drawing (left) and chemical structure (right) of (2′*R*)-(*M*)-*trans*-**1a**.

Enantioresolution of (±)-*trans*-1a and (±)-*cis*-2a by Chiral HPLC. Enantioresolution of (±)-*trans*-**1a** and (±)-*cis*-**2a** was performed by preparative chiral HPLC (Chiralpak OD) under normal phase conditions using heptane:2-propanol = 99:1 as eluent mixture at room temperature. The combined solutions of second-eluted enantiomer of *trans*-**1a** were evaporated under reduced pressure, and the residue was recrystallized from *n*-hexane to give colorless prisms suitable for X-ray crystallographic analysis. Crystals of enantiomers of *cis*-**2a** suitable for X-ray analysis could not be obtained so far.

X-ray Crystallographic Analysis of (2′*R*)-(*M*)-*trans*-1a. A single crystal of enantiomerically pure *trans*-**1a** was subjected to X-ray analysis. The crystal was found to be orthorhombic: space group $P2_12_12_1$. The absolute configuration of this enantiomer was determined to be (2′*R*)-(*M*) by Flack's[25] *x*-refinement ($x = -0.07(7)$). This X-ray analysis demonstrated that the methyl substituent at the 2′-position adopted a pseudoaxial orientation to minimize steric hindrance, which is in accordance with the results of the ^{1}H NMR study (Figure 6 and Table 2). The geometry of (2′*R*)-(*M*)-*trans*-**1a** in the solid state is characterized as follows: central double bond, C(1′)−C(9) =

(21) Oosterling, M. L. C. M.; Schoevaars, A. M.; Haitjema, H. J.; Feringa, B. L. *Isr. J. Chem.* **1996**, *36*, 341−348.
(22) (a) Vasiliu, G.; Rasanu, N.; Maior, O. *Rev. Chim. (Bucharest)* **1968**, *19(10)*, 561−565; *Chem. Abstr.* **1969**, *71*, 38739. (b) Schönberg, A.; Sidky, M. M. *J. Am. Chem. Soc.* **1959**, *81*, 2259−2262. (c) Schönberg, A.; Stolpp, T. *Ber.* **1930**, *63*, 3102−3116.
(23) (a) Barton, D. H. R.; Willis, B. J. *J. Chem. Soc., Perkin Trans. 1* **1972**, 305−310. (b) Buter, J.; Wassenaar, S.; Kellogg, R. M. *J. Org. Chem.* **1972**, *37*, 4045−4060.
(24) It should be noted that due to the distinct upper and lower halves in the second generation molecular motor, the McMurry olefinization used for synthesis of the first generation molecular motors is less suitable, whereas other olefinization methods failed due to severe steric hindrance during the coupling reaction.
(25) (a) Flack, H. D. *Acta Crystallogr.* **1983**, *A39*, 876−881. (b) Flack, H. D.; Bernardinelli, G. *Acta Crystallogr.* **1999**, *A55*, 908−915.

Table 2. X-ray Crystallographic Data of (2′*R*)-(*M*)-*trans*-**1a**, Racemic (2′*R**)-(*P**)-*trans*-**1b**, Racemic (2′*S**)-(*M**)-**8a**, Racemic (2′*S**)-(*M**)-**9a**

compound	(2′*R*)-(*M*)-*trans*-**1a**	(2′*R**)-(*P**)-*trans*-**1b**	(2′*S**)-(*M**)-**8a**	(2′*S**)-(*M**)-**9a**
formula	$C_{28}H_{22}OS_2$	$C_{28}H_{22}OS_2$	$C_{31}H_{28}$	$C_{30}H_{24}$
fw (g/mol)	438.61	438.61	400.56	384.52
crystal dimension	0.25 × 0.33 × 0.38	0.50 × 0.50 × 0.40	0.45 × 0.33 × 0.15	0.50 × 0.42 × 0.02
crystal system	orthorhombic	monoclinic	triclinic	monoclinic
space group	$P2_12_12_1$	$P2_1/c$	$\bar{P}1$	$P2_1/c$
a (Å)	10.201(1)	14.570(1)	10.034(2)	10.0860(7)
b (Å)	12.274(1)	7.376(1)	10.307(2)	12.8725(9)
c (Å)	17.431(1)	20.858(1)	11.566(2)	16.812(1)
α (deg)			100.089(3)	
β (deg)		100.904(5)	102.135(3)	96.261(1)
γ (deg)			101.110(4)	
V (Å^3)	2182.5(3)	2201.1(4)	1118.1(4)	2169.7(2)
Z	4	4	2	4
D_{calc} (g/cm^3)	1.335	1.324	1.190	1.177
T (K)	295	130	293	293
μ (cm^{-1})	2.62	2.60	0.67	0.66
number of reflections	4735	4783	5019	4949
number of refined parameters	367	368	392	367
final agreement factor				
w*R*(*F* ^{2})	0.0992	0.1311	0.0911	0.1267
R(*F*)	0.0381	0.0440	0.0391	0.0452
absolute-structure parameter Flack's **x**	0.07(7)			

1.351 Å; bond angles around central double bond, C(8a)−C(9)−C(9a) = 113.22°, C(8a)−C(9)−C(1′) = 121.73°, C(9a)−C(9)−C(1′) = 124.97° (total angle around C(9) is 359.92°), C(10′b)−C(1′)-C(2′) = 111.30°, C(10′b)−C(1′)−C(9) = 123.12°, C(2′)−C(1′)−C(9) = 125.48° (total angle around C(1′) is 359.90°); the dihedral angle between the naphthalene plane of the upper part and the central double bond, C(10′a)−C(10′b)−C(1′)−C(9) = −56.5°; dihedral angles between the thioxanthene arene moieties of the lower part and the central double bond, C(1)−C(9a)−C(9)−C(1′) = 51.3°, C(8)−C(8a)−C(9)−C(1′) = −47.7°; dihedral angles at the central double bond, C(8a)−C(9)−C(1′)−C(10′b) = 0.2°, C(9a)−C(9)−C(1′)−C(2′) = −7.1° (average value is −3.44°), C(8a)−C(9)−C(1′)−C(2′) = 176.85°, C(9a)−C(9)−C(1′)−C(10′b) = 176.26° (average value is 176.56°). The central double bond is therefore a little twisted, although each sp^2 carbon of the central double bond maintains its planar structure. The lower thioxanthene part of the molecule adopts a folded structure[26] to diminish the steric strain around the central double bond and, together with the pseudo-boat conformation of the thiopyran ring of the upper part, is responsible for the helical shape of the entire molecule.

Photochemistry of *trans*-1a and *cis*-2a and X-ray Crystallographic Analysis of Racemic Less-Stable (2′*R)-(*P**)-*trans*-1b.** To examine the photochemical and thermal behavior of the overcrowded alkenes *trans*-**1a** and *cis*-**2a**, we initially irradiated both racemic trans- and cis-isomers and monitored the progress of the reaction by ^{1}H NMR (Scheme 3). Irradiation of a solution of 25 mg of racemic *trans*-**1a** in 3 mL of *n*-hexane-dichloromethane (10:1) was performed by a high-pressure mercury lamp using a 365 nm filter (bandwidth = 10 nm, Ø = 5 cm) at 10 °C. Solvents were evaporated under reduced pressure to give white solids, which were directly subjected to ^{1}H NMR measurements. A 14:86 ratio of starting material (*trans*-**1a**):product (*cis*-**2b**) was observed. The ^{1}H NMR spectrum of product *cis*-**2b** revealed that the absorption of the methyl substituent at the 2′-position was shifted downfield to 1.10 ppm, and the signal of the proton at the 2′-position appeared to have

Scheme 3

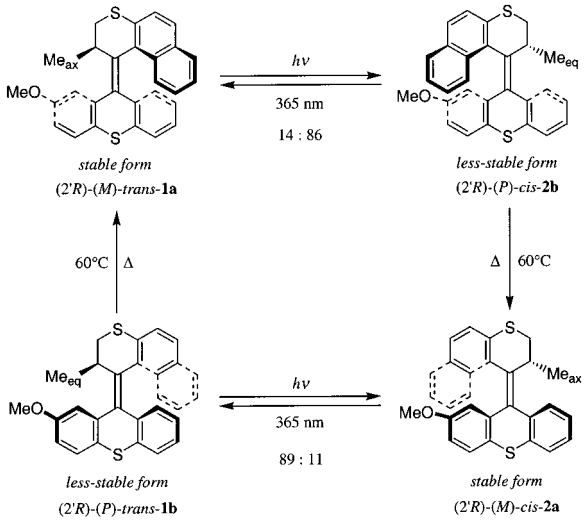

shifted upfield to 2.76 ppm (Table 1). Notably, the absorption of the methoxy group at the lower part was shifted upfield to 2.99 ppm due to shielding by the naphthalene moiety (Table 1), which indicates that trans to cis isomerization occurred by irradiation. Coupling constants of 12.4 and 7.3 Hz were found for H(2′) and H(3′) (Table 1), which proved that the methyl substituent at the 2′-position adopts a pseudoequatorial orientation as was confirmed by X-ray analysis (vide infra). The obtained *cis*-**2b** isomer is supposed to be less stable because of the steric hindrance between the methyl group and the thioxanthene lower part as indicated by molecular modeling studies (Figure 5). Irradiation of a solution of 25 mg of racemic *cis*-**2a** in 3 mL of *n*-hexane-dichloromethane (10:1) was performed under the same conditions, and subsequent evaporation of solvents gave a white solid (Scheme 3). An 11:89 ratio of starting material (*cis*-**2a**):product (*trans*-**1b**) was found. The ^{1}H NMR spectrum of the photochemical product *trans*-**1b** showed that absorptions of the methyl group and the proton at the 2′-position were found at 1.17 and 2.74 ppm, respectively (Table 1). It is again remarkable that the absorption of the methoxy group at the lower part was shifted downfield to 3.85 ppm due

(26) Biedermann, P. U.; Stezowski, J. J.; Agranat, I. *Eur. J. Org. Chem.* **2001**, 15−34 and references therein.

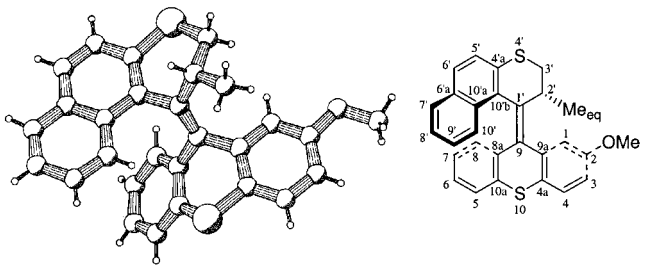

Figure 7. PLUTO drawing (left) and chemical structure (right) of (2′*R**)-(*P**)-*trans*-**1b**.

to escaping from shielding by the naphthalene moiety (Table 1) in accordance with a trans-geometry. The coupling constants of H(2′) and H(3′) were found to be 12.1 and 7.3 Hz (Table 1), which indicated that the methyl substituent at the 2′-position adopts a pseudoequatorial orientation. The trans-isomer **1b** is expected to be less stable, as compared to trans-isomer **1a**, because of the steric hindrance between the methyl group and the thioxanthene lower part as indicated by molecular modeling studies (Figure 4).

Heating of each solution of less-stable isomers, *trans*-**1b** and *cis*-**2b**, in *n*-hexane at 60 °C resulted in quantitative conversion into stable isomers, *trans*-**1a** and *cis*-**2a**, respectively, as was evident from ^{1}H NMR. It should be emphasized that thermal trans−cis isomerization does not occur in this system.

To determine unequivocally the stereostructure of the less-stable forms of these olefins, attempts were undertaken to obtain crystals of *trans*-**1b** and *cis*-**2b**. After irradiation, solutions both of *trans*-**1a** and of *cis*-**2a** in *n*-hexane-dichloromethane solvents were partly evaporated under reduced pressure at 10 °C. The concentrated solutions were allowed to stand overnight at 5 °C. Crystals of racemic *trans*-**1b** were obtained suitable for X-ray crystallographic analysis. A single crystal of racemic less-stable *trans*-**1b** was found to be monoclinic: space group $P2_1/c$ (Table 2). As shown in Figure 7, the relative configuration of less-stable *trans*-**1b** was determined to be (2′*R**)-(*P**), and the methyl substituent at the 2′-position clearly adopts a pseudoequatorial orientation, which is in accordance with the results of the ^{1}H NMR study. The geometrical characteristics of less-stable *trans*-**1b** in the solid state are summarized as follows: central double bond, C(1′)−C(9) = 1.340 Å; bond angles around central double bond, C(8a)−C(9)−C(9a) = 111.33°, C(8a)−C(9)−C(1′) = 121.81°, C(9a)−C(9)−C(1′) = 126.74° (total angle around C(9) is 359.88°), C(10′b)−C(1′)−C(2′) = 108.45°, C(10′b)−C(1′)−C(9) = 122.83°, C(2′)−C(1′)−C(9) = 128.60° (total angle around C(1′) is 359.88°); the dihedral angle between the naphthalene plane of the upper part and the central double bond, C(10′a)−C(10′b)−C(1′)−C(9) = 62.8°; dihedral angles between the thioxanthene arene moieties of the lower part and the central double bond, C(1)−C(9a)−C(9)−C(1′) = −59.4°, C(8)−C(8a)−C(9)−C(1′) = 52.7°; dihedral angles of the central double bond, C(8a)−C(9)−C(1′)−C(10′b) = −8.9°, C(9a)−C(9)−C(1′)−C(2′) = 0.0° (average value is −4.46°), C(8a)−C(9)−C(1′)−C(2′) = 175.58°, C(9a)−C(9)−C(1′)−C(10′b) = 175.52° (average value is 175.54°). These geometrical parameters are almost similar to those of (2′*R*)-(*M*)-*trans*-**1a**.

CD Studies of Unidirectional Rotation Behavior of *trans*-1 and *cis*-2. The photochemical trans−cis and cis−trans isomerizations and the thermal isomerization steps were also examined by CD spectroscopy using the enantiomers of *trans*-**1** and *cis*-**2**. CD spectra of (2′*R*)-(*M*)-*trans*-**1a** and (2′*S*)-(*P*)-*cis*-**2a** are shown in Figure 8A[27] and C.[28] Irradiation of the solutions of (2′*R*)-(*M*)-*trans*-**1a** and (2′*S*)-(*P*)-*cis*-**2a** in *n*-hexane (concentration of the solution: 3.0×10^{-5} M) by a high-pressure mercury lamp using a 365 nm filter (bandwidth = 10 nm, Ø = 5 cm) at 10 °C for 1 h resulted in formation of less-stable (2′*R*)-(*P*)-*cis*-**2b** and (2′*S*)-(*M*)-*trans*-**1b**, respectively. The photochemical trans−cis (cis−trans) isomerization induced an *M* to *P* (*P* to *M*) helicity inversion (Figure 8, trace A to B and trace C to D). Furthermore, because several clear isosbestic points were observed in both CD and UV spectra, no degradation and/or side reaction occurred in this photochemical trans−cis (cis−trans) isomerization.

Starting with the solution of stable (2′*R*)-(*M*)-*trans*-**1a** in *n*-hexane, we next examined the sequential isomerizations including thermal conversions. When the temperature of the solution of less-stable (2′*R*)-(*P*)-*cis*-**2b**, obtained after irradiation of (2′*R*)-(*M*)-*trans*-**1a**, was raised to 60 °C, complete conversion to (2′*R*)-(*M*)-*cis*-**2a** was observed, and the concomitant change in CD absorption confirmed the helix reversal, from *P* to *M* helicity, associated with this thermal interconversion (Figure 9, trace B to C). Subsequent irradiation of the solution of (2′*R*)-(*M*)-*cis*-**2a** in *n*-hexane resulted in formation of (2′*R*)-(*P*)-*trans*-**1b**. The change in sign of CD absorption again indicated that an *M* to *P* helicity inversion occurred in the photochemical cis to trans isomerization (Figure 9, trace C to D). When the temperature of this solution was raised to 60 °C, a complete conversion to (2′*R*)-(*M*)-*trans*-**1a** was observed, and the CD absorption again changed signs (Figure 9, trace D to A). The inset at Figure 9 shows the change of $\Delta\epsilon$ value at 272 nm as monitored during three full cycles clearly demonstrating the repetitive nature of the rotary motion. After three cycles, a mixture of (2′*R*)-(*M*)-*trans*-**1a**/(2′*R*)-(*M*)-*cis*-**2a** with a ratio of approximately 6:4 was observed due to the photoequilibria. However, this does not affect the repetitive unidirectional behavior of the motor molecules, and each photochemical and thermal step still implies a helix inversion. No thermal cis−trans isomerizations were observed as long as the thermal conversions were performed in the dark excluding any concomitant photochemical process. These CD studies confirm that both *trans*-**1a** and *cis*-**2a** are the stable forms of these compounds (with a pseudoaxial methyl substituent) and that photochemically they are converted into the less-stable isomers *cis*-**2b** and *trans*-**1b** (with a pseudoequatorial methyl substituent), respectively.

Scheme 3 summarizes the different stereoisomers and the dynamic processes that are observed starting with (2′*R*)-(*M*)-*trans*-**1a**. The experimental results show that the upper naphthothiopyran part undergoes a full 360° rotation around the central double bond in a counterclockwise sense relative to the lower thioxanthene part. Two photochemical conversions are both energetically uphill processes and generate the less-stable isomers {(2′*R*)-(*P*)-*cis*-**2b** and (2′*R*)-(*P*)-*trans*-**1b**} with the less favorable equatorial orientation of the methyl substituents at the 2′-position. Each photochemical step is followed by an energetically downhill process generating stable isomers {(2′*R*)-

(27) (2′*R*)-(*M*)-*trans*-**1a**: UV (*n*-hexane) λ_{max} 325 (ϵ 8300), 259 (35 100), 222 (51 300), CD (*n*-hexane) λ_{ext} 349.8 nm ($\Delta\epsilon$ +19.1), 318.6 (+15.4), 277.2 (−155.4), 253.0 (+40.8), 223.8 (+98.1).

(28) (2′*S*)-(*P*)-*cis*-**2a**: UV (*n*-hexane) λ_{max} 321 (ϵ 7400), 266 (28 200), 248 (29 100), 213 (50 500), CD (*n*-hexane) λ_{ext} 356.8 nm ($\Delta\epsilon$ −14.7), 325.4 (+2.7), 276.4 (+120.6), 252.2 (−76.1), 223.2 (−92.4).

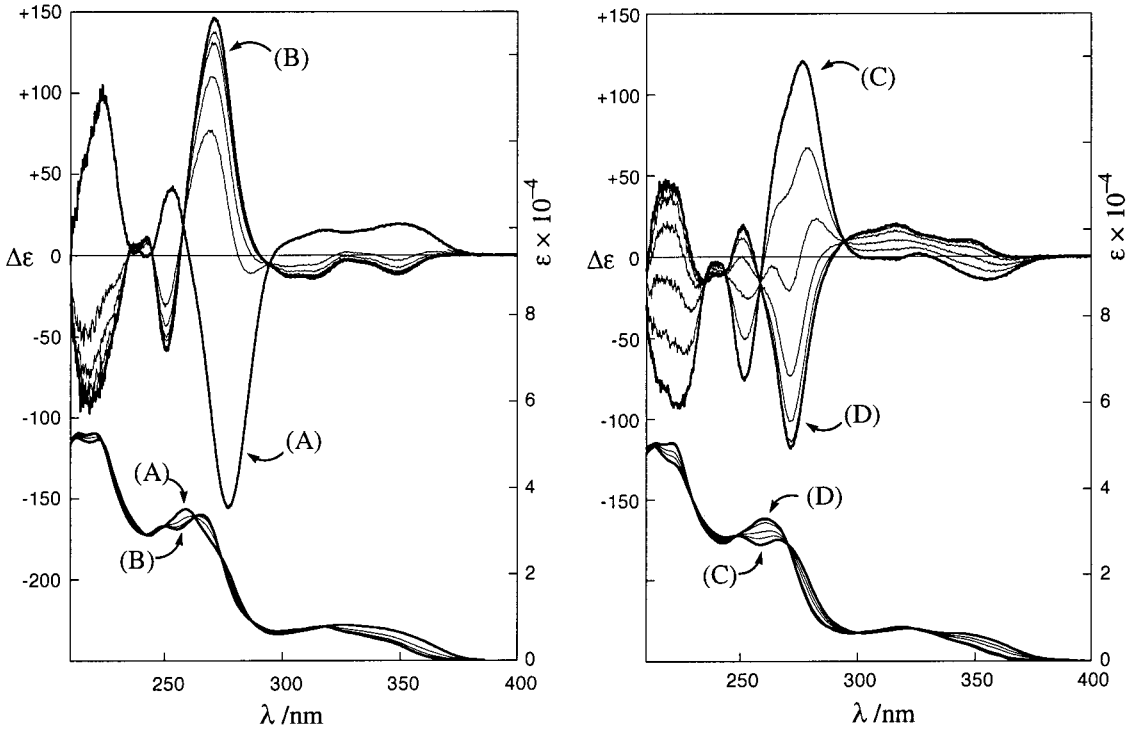

Figure 8. CD and UV spectra of (2′*R*)-*trans*-**1** and (2′*S*)-*cis*-**2** and change in CD and UV upon irradiation and the inversion of sign of Cotton effects during irradiation. (A) stable (2′*R*)-(*M*)-*trans*-**1a**, (B) less-stable (2′*R*)-(*P*)-*cis*-**2b**, (C) stable (2′*S*)-(*P*)-*cis*-**2a**, (D) less-stable (2′*S*)-(*M*)-*trans*-**1b**.

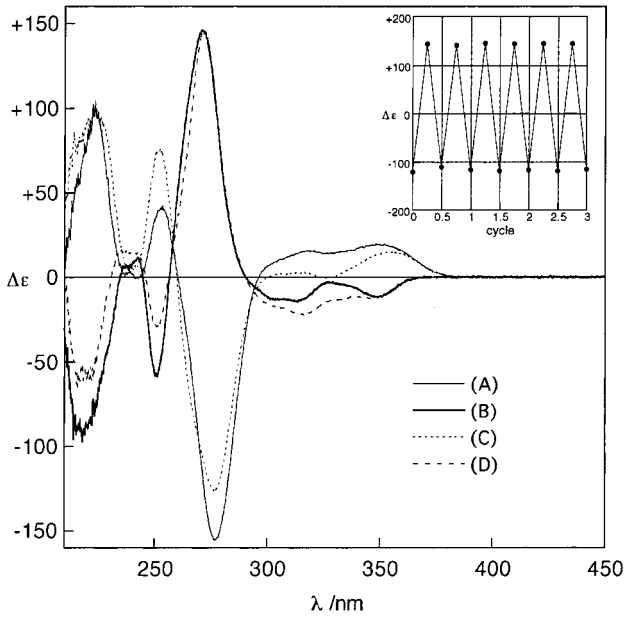

Figure 9. CD spectra of each of the four stages of rotation. Trace A, (2′*R*)-(*M*)-*trans*-**1a**; Trace B, (2′*R*)-(*P*)-*cis*-**2b**; Trace C, (2′*R*)-(*M*)-*cis*-**2a**; Trace D, (2′*R*)-(*P*)-*trans*-**1b**. Inset, changes in Δϵ value during full rotation cycle monitoring at 272 nm.

(*M*)-*cis*-**2a** and (2′*R*)-(*M*)-*trans*-**1a**}. As anticipated, during the two thermal steps the methyl substitutent adopts the more favorable axial orientation, and the reverse rotation pathway is effectively blocked. At the appropriate wavelength (365 nm) and temperature (60 °C), a continuous unidirectional rotation is induced in this second generation molecular motor. The most remarkable finding is that a single stereogenic center at the 2′-position controls the direction of rotary motion in this system.

Structural Modification To Tune the Speed of Rotary Motion. One of the envisioned key features of the second generation of molecular motors is the ability to tune the speed of the thermal conversion by varying atoms X and Y (Figure 3). As discussed above, the two thermal steps during the rotation cycle proceed quantitatively due to the significant difference between the ground-state energies of the stable (*trans*-**1a** and *cis*-**2a**) and less-stable forms (*trans*-**1b** and *cis*-**2b**). Despite being energetically downhill processes, thermal energy is required to pass the energy barrier (Gibbs energy of activation; $\Delta G^{\ddagger}$) associated with these processes. The speed of rotary motion is largely correlated with the Gibbs energy of activation ($\Delta G^{\ddagger}$) of the thermal conversions. During the thermal process, the upper and lower part move along each other, and the rate of this movement heavily depends on the steric hindrance in the fjord region of the molecule. As a consequence, the larger the bridging atoms X and Y and the longer the bond lengths with their adjacent carbon atoms, the more the upper and lower part are pushed toward each other resulting in higher Gibbs energies of activation ($\Delta G^{\ddagger}$) for the thermal steps.

To investigate the possibility to tune the energy barriers of the thermal conversion, seven new molecular motors **3**−**9** were designed (Figure 3). It is emphasized that, in contrast with the second generation motors *trans*-**1** and *cis*-**2**, this series of seven new molecular motors has symmetric lower parts ($R_1 = R_2$). This feature implies that one photochemical and subsequent thermal step reverts the molecule to the starting compound (see also Scheme 8).

Synthesis of Molecular Motors with Symmetric Lower Parts. The seven new molecular motors **3**−**9** contain chiral 2,3-dihydro-2-methylnaphtho[2,1-*b*]thiopyran or 2,3-dihydro-3-methylphenanthrene upper parts and several types of symmetric lower parts. The synthesis of 2,3-dihydro-2-methyl-1*H*-naphtho-[2,1-*b*]thiopyran-1-one hydrazone **13** is described in Scheme 1. The synthesis of the upper part precursor 2,3-dihydro-3-methyl-4(1*H*)-phenanthrenone hydrazone **18** was performed by

Scheme 4[a]

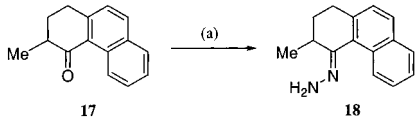

17 18

[a] (a) $H_2NNH_2 \cdot H_2O$/EtOH, reflux, 94%.

Scheme 5[a]

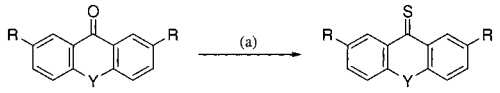

19: Y=S, R=H
20: Y=S, R=OMe
21: Y=O, R=H
22: Y=$C(CH_3)_2$, R=H
23: Y=CHCH, R=H

24: Y=S, R=H
25: Y=S, R=OMe
26: Y=O, R=H
27: Y=$C(CH_3)_2$, R=H
28: Y=CHCH, R=H

[a] (a)P_2S_5/toluene, reflux.

Scheme 6[a]

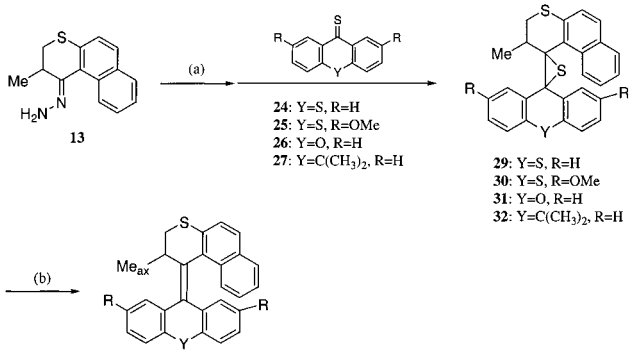

13

24: Y=S, R=H
25: Y=S, R=OMe
26: Y=O, R=H
27: Y=$C(CH_3)_2$, R=H

29: Y=S, R=H
30: Y=S, R=OMe
31: Y=O, R=H
32: Y=$C(CH_3)_2$, R=H

3a: Y=S, R=H
4a: Y=S, R=OMe
5a: Y=O, R=H
6a: Y=$C(CH_3)_2$, R=H

[a] (a) Ag_2O, $MgSO_4$, KOH (sat sol)/MeOH/CH_2Cl_2, 0 °C, 30−73%; (b) Cu-bronze/*p*-xylene, reflux, 85−99%.

refluxing ketone **17**, which is a precursor of the first light-driven molecular motor,[29] in ethanol with a large excess of hydrazine monohydrate (Scheme 4). The lower parts, five different thioketones **24**−**28**,[22] were prepared by refluxing ketones **19**−**23**[30] in toluene with an excess of phosphorus pentasulfide (Scheme 5).

To prepare motors **3a**−**6a**, hydrazone **13** was oxidized to the corresponding diazo-intermediate with silver(I) oxide (2 equiv) in dichloromethane at −5 to 0 °C, and subsequent addition of the appropriate thioketones **24**−**27** gave episulfides **29**−**32** in moderate yields (30−73%). Desulfurization of episulfides **29**−**32** by reflux in *p*-xylene in the presence of copper bronze provided olefins **3a**−**6a** in high yields (85−99%) (Scheme 6). The oxidation of hydrazone **18** was relatively slow using silver(I) oxide, and 4 equiv of silver(I) oxide was needed. The unstable deep red diazo-compound was added to the appropriate thioketones **24**, **27**, or **28** to give episulfides **33**−**35** in rather low yields (10−23%). Desulfurization of episulfides **33** and **34** by refluxing in *p*-xylene in the presence of copper bronze gave olefins **7a** and **8a** in fair yields (63−83%) (Scheme 7). The desulfurization reaction of episulfide **35** demanded triphenylphosphine in refluxing toluene to provide olefin **9a** in a 54% yield (Scheme 7).

Scheme 7[a]

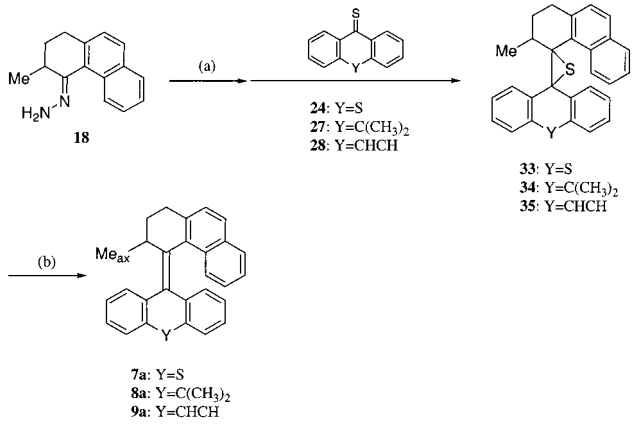

18

24: Y=S
27: Y=$C(CH_3)_2$
28: Y=CHCH

33: Y=S
34: Y=$C(CH_3)_2$
35: Y=CHCH

7a: Y=S
8a: Y=$C(CH_3)_2$
9a: Y=CHCH

[a] (a) Ag_2O, $MgSO_4$, KOH (sat sol)/MeOH/CH_2Cl_2, 0 °C, 10−23%; (b) Cu-bronze/*p*-xylene, reflux (**7a** and **8a**), 63-83% or PPh_3/toluene, reflux (**9a**), 54%.

Table 3. Selected ^{1}H NMR Data of Molecular Motors **3a**−**9a** in $CDCl_3$

stable forms	chemical shift (ppm): methyl group, Me_{ax}	chemical shift (ppm): H(2′) (**3a**–**6a**), H(3′) (**7a**–**9a**)	coupling constant (Hz) $J_{H(2')-H(3')}$
3a	0.78 (0.53[a])	4.13 (3.98[a])	7.3, 2.9
4a	0.82 (0.58[a])	4.20 (4.12[a])	7.7, 3.3
5a	0.79 (0.53[b])	4.29 (4.08[b])	7.0, 2.6
6a	0.82 (0.63[a])	4.41 (4.31[a])	8.8, 3.3
7a	0.82 (0.55[a])	3.90 (3.91[a])	8.4, 4.0
8a	0.65 (0.62[a])	4.10 (4.16[a])	9.3, 2.8
9a	0.57 (0.57[a])	3.46 (3.54[a])	9.0, 5.5

[a] Solvent was toluene-d_8. [b] Solvent was benzene-d_6.

Stereochemistry of New Molecular Motors. To determine the configuration of the methyl substituent at the 2′-position in **3a**−**6a** or the 3′-position in **7a**−**9a**, the ^{1}H NMR spectra were studied in detail. As shown in Table 3, the coupling constants of H(2′) and H(3′)[31] of olefins **3a**−**7a** were observed in the range of 7.0−8.8 Hz and 2.6−4.0 Hz, which proves that the methyl substituents of **3a**−**7a** adopt a pseudoaxial orientation akin to the first "second generation" motor (*trans*-**1a** and *cis*-**2a**, Table 1). However, the coupling constants of H(2′) and H(3′) of olefins **8a** and **9a** were found to be 9.3, 2.8 Hz (**8a**) and 9.0, 5.0 Hz (**9a**), respectively. On the basis of these data, it was indefinite that the methyl groups of **8a** and **9a** also adopt a pseudoaxial orientation. Ultimately we could determine the preferred conformation of the methyl groups of **8a** and **9a** by X-ray crystallographic analyses.

Recrystallization of racemic **8a** from *n*-hexane yielded a single crystal suitable for X-ray analysis. The crystal was found to be triclinic: space group $P\bar{1}$. A single crystal of racemic **9a** was obtained by recrystallization from diethyl ether and found to be monoclinic: space group $P2_1/c$. As shown in Figures 10 and 11, the X-ray studies demonstrated that (i) the methyl substituents at the 3′-position adopt a pseudoaxial orientation in both cases, (ii) each cyclohexene ring of the upper part has a boatlike conformation to minimize steric hindrance between the upper and lower part, and (iii) both lower parts of **8a** and **9a** adopt folded structures[26] similar to the first "second generation" molecular motor (*trans*-**1a**, Figure 6 and Table 2).

(29) Harada, N.; Koumura, N.; Feringa, B. L. *J. Am. Chem. Soc.* **1997**, *119*, 7256−7264.
(30) See Experimental Section for synthesis of ketone **20**. Ketone **20** was synthesized according to Falshaw, C. P.; Hashi, N. A.; Taylor, G. A. *J. Chem. Soc., Perkin Trans. 1* **1985**, 1837−1843.
(31) Following IUPAC regulations, different numbering schemes are adopted for the thiopyran upper part, on one hand, and phenanthrene upper part, on the other hand (see Figures 6, 7, 10, and 11).

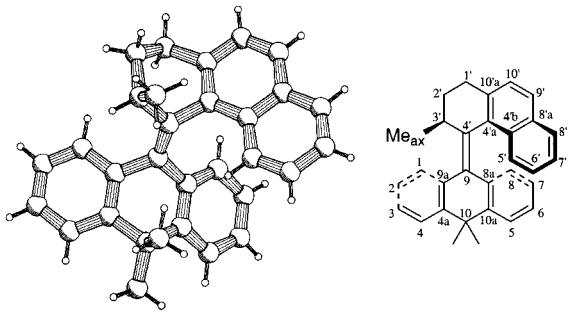

Figure 10. PLUTO drawing (left) and chemical structure (right) of (2′*S**)-(*M**)-**8a**.

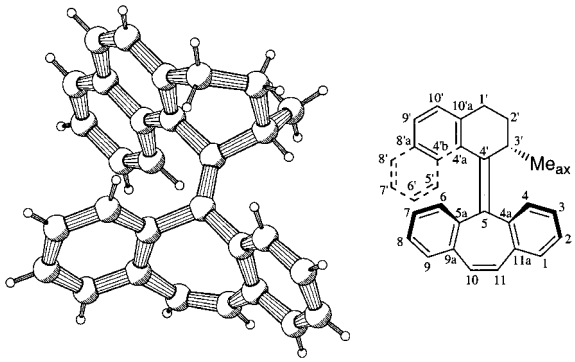

Figure 11. PLUTO drawing (left) and chemical structure (right) of (2′*S**)-(*M**)-**9a**.

Moreover, all X-ray analyses (*trans*-**1a**, *trans*-**1b**, **8a**, and **9a**) confirm identical helical structures for these compounds.

The geometry of racemic **8a** in the solid state is characterized as follows: central double bond, C(4′)−C(9) = 1.3436 Å; bond angles around the central double bond, C(8a)−C(9)−C(9a) = 111.28°, C(8a)−C(9)−C(4′) = 124.24°, C(9a)−C(9)−C(4′) = 124.46° (total angle around C(9) is 359.98°), C(4′a)−C(4′)−C(3′) = 109.58°, C(4′a)−C(4′)−C(9) = 125.80°, C(3′)−C(4′)−C(9) = 124.29° (total angle around C(4′) is 359.67°); the dihedral angle between the naphthalene plane of the upper part and the central double bond, C(4′b)−C(4′a)−C(4′)−C(9) = −65.37°; dihedral angles between arene moieties of the lower part and the central double bond, C(1)−C(9a)−C(9)−C(4′) = 46.62°, C(8)−C(8a)−C(9)−C(4′) = −43.28°; dihedral angles of the central double bond, C(8a)−C(9)−C(4′)−C(4′a) = 12.48°, C(9a)−C(9)−C(4′)−C(3′) = 3.47° (average value is 7.97°), C(8a)−C(9)−C(4′)−C(3′) = −174.76°, C(9a)−C(9)−C(4′)−C(4′b) = −169.30° (average value is −172.03°).

The geometrical characteristics of racemic **9a** in the solid state are summarized as follows: central double bond, C(4′)−C(5) = 1.3485 Å; bond angles around the central double bond, C(5a)−C(5)−C(4a) = 114.25°, C(5a)−C(5)−C(4′) = 121.96°, C(4a)−C(5)−C(4′) = 123.62° (total angle around C(5) is 359.83°), C(4′a)−C(4′)−C(3′) = 112.06°, C(4′a)−C(4′)−C(5) = 123.19°, C(3′)−C(4′)−C(5) = 124.36° (total angle around C(4′) is 359.61°); the dihedral angle between the naphthalene plane of the upper part and the central double bond, C(4′b)−C(4′a)−C(4′)−C(5) = −62.39°; dihedral angles between arene moieties of the lower part and the central double bond, C(4)−C(4a)−C(5)−C(4′) = 60.09°, C(6)−C(5a)−C(5)−C(4′) = −57.20°; dihedral angles of the central double bond, C(5a)−C(5)−C(4′)−C(4′a) = −0.67°, C(4a)−C(5)−C(4′)−C(3′) = −3.29° (average value is −1.98°), C(5a)−C(5)−C(4′)−C(3′) = 171.69°, C(4a)−C(5)−C(4′)−C(4′a) = −175.65° (average value is −1.98°).

Photochemistry of the Motors 3a−9a and Structural Aspects of Less-Stable Motors 3b−9b. To examine the rate of the thermal step, new motors **3a−9a** were first converted into their less-stable isomers **3b−9b** (Scheme 8). Irradiations of solutions of **3a−9a** in toluene-d_8 or benzene-d_6 were carried out in NMR tubes with a high-pressure mercury lamp using a Pyrex or a 365 nm filter at room temperature or −25 °C. Specific conditions of the irradiation experiments are summarized in Table 4. Ratios of stable and less-stable isomers in the photostationary state (PSS, definite equilibrium) were calculated from the integral values of methyl substituents of the isomers, which have distinct chemical shifts in the ^{1}H NMR spectra (Tables 3 and 5). The photostationary states were attained by irradiation within 3 h for olefins **3**, **4**, and **6** (Table 4, entries 1, 2, and 4) in fair ratios, while irradiation for 24 h was required for reaching the photoequilibrium of olefin **5** (Table 4, entry 3). Longer irradiation time was required since light of lower intensity, due to the 365 nm filter, was applied.[32] High diastereoselectivities were reached in the photoisomerization of motors **3−6**. Excellent and near-perfect photoequilibria of 1:99 were established for motors **7** and **8**, which have a 2,3-dihydro-3-methylphenanthrene upper part (Table 4, entries 5 and 6). In both cases, irradiations were performed at −25 °C since low activation energies of the thermal conversions were expected which, at room temperature, seriously would harm the ratios at the photostationary states. Finally, motor **9** demanded a long irradiation time of 168 h after which a reasonable equilibrium of 25:75 was ascertained (Table 4, entry 7). Clean photochemical isomerization was observed in all cases, and the less-stable isomers **3b−9b** could be characterized by NMR.

In cases of **3b−8b**, large coupling constants between H(2′) and H(3′)[31] protons, which were attributed to the diaxial orientation, were observed (Table 5). These results reveal that each methyl substituent of **3b−8b** was proven to adopt a pseudoequatorial orientation. Although the coupling constants between H(2′) and H(3′) of **9b** were relatively small as compared to those of the other motors (Table 5), the methyl group of **9b** was presumed to have a pseudoequatorial orientation as well.

Kinetic Studies of the Thermal Conversions by ^{1}H NMR Spectroscopy. With less-stable motors **3b−6b** and **9b** in hand, detailed kinetic studies of the first-order thermal decay into their respective stable isomers **3a−6a** and **9a** were executed (Scheme 8). The decay of less-stable isomers **3b−6b** and **9b** was monitored by ^{1}H NMR. The isomerization of the less-stable isomers **3b−6b** and **9b** and the exclusive formation of the stable isomers **3a−6a** and **9a** could be determined quantitatively by the integration of the distinct absorptions of the methyl substituents.

The straight lines obtained by plotting the natural log of decay of less-stable isomers **3b−6b** and **9b** versus time confirm the first-order nature of the thermal step of these motors. The reaction rate (k), half-life time ($t_{1/2}$), and Gibbs energy of activation ($\Delta G^{\ddagger}$) at each specific temperature were obtained

(32) It should be noted that irradiation times strongly depend on concentration, filters, and light sources used. The intrinsic photochemical trans−cis isomerization is extrmely fast. Zijlstra, R. W. J.; van Duijnen, P. T; Feringa, B. L.; Steffen, T.; Duppen, K.; Wiersma, D. A. *J. Phys. Chem. A* **1997**, *101*, 9828−9836. See also: Zijlstra, R. W. J. Excited State Charge Separation in Symmetrical Alkenes. Ph.D. Thesis, Groningen, 2001; Chapter 5.

Scheme 8

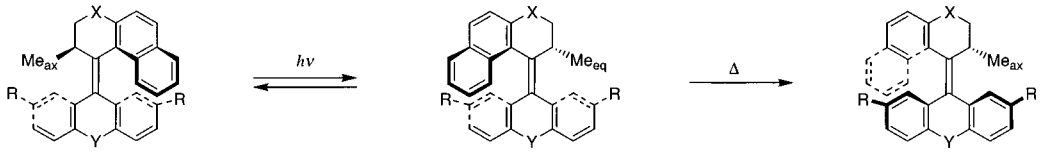

(2′*R**)-(*M**)-**3a**: X=S, Y=S, R=H
(2′*R**)-(*M**)-**4a**: X=S, Y=S, R=OMe
(2′*R**)-(*M**)-**5a**: X=S, Y=O, R=H
(2′*R**)-(*M**)-**6a**: X=S, Y=C(CH$_3$)$_2$, R=H
(2′*S**)-(*M**)-**7a**: X=CH$_2$, Y=S, R=H
(2′*S**)-(*M**)-**8a**: X=CH$_2$, Y=C(CH$_3$)$_2$, R=H
(2′*S**)-(*M**)-**9a**: X=CH$_2$, Y=CHCH, R=H

(2′*R**)-(*P**)-**3b**: X=S, Y=S, R=H
(2′*R**)-(*P**)-**4b**: X=S, Y=S, R=OMe
(2′*R**)-(*P**)-**5b**: X=S, Y=O, R=H
(2′*R**)-(*P**)-**6b**: X=S, Y=C(CH$_3$)$_2$, R=H
(2′*S**)-(*P**)-**7b**: X=CH$_2$, Y=S, R=H
(2′*S**)-(*P**)-**8b**: X=CH$_2$, Y=C(CH$_3$)$_2$, R=H
(2′*S**)-(*P**)-**9b**: X=CH$_2$, Y=CHCH, R=H

(2′*R**)-(*M**)-**3a**: X=S, Y=S, R=H
(2′*R**)-(*M**)-**4a**: X=S, Y=S, R=OMe
(2′*R**)-(*M**)-**5a**: X=S, Y=O, R=H
(2′*R**)-(*M**)-**6a**: X=S, Y=C(CH$_3$)$_2$, R=H
(2′*S**)-(*M**)-**7a**: X=CH$_2$, Y=S, R=H
(2′*S**)-(*M**)-**8a**: X=CH$_2$, Y=C(CH$_3$)$_2$, R=H
(2′*S**)-(*M**)-**9a**: X=CH$_2$, Y=CHCH, R=H

Table 4. Results of Irradiation Experiments[a] of Motors **3a**−**9a**

entry	motor	filter	concentration (mol/L)	time (h)	temp (°C)	product	ratio of PSS[c]
1	**3a**	Pyrex	7.35×10^{-2}	3	20	**3b**	8:92
2	**4a**	Pyrex	7.12×10^{-2}	3	20	**4b**	13:87
3	**5a**[b]	365 nm	5.10×10^{-2}	24	20	**5b**	23:77
4	**6a**	Pyrex	5.97×10^{-2}	2	20	**6b**	8:92
5	**7a**	Pyrex	3.41×10^{-2}	17	−25	**7b**	1:99
6	**8a**	Pyrex	3.27×10^{-2}	17	−25	**8b**	1:99
7	**9a**	Pyrex	3.61×10^{-2}	168	20	**9b**	25:75

[a] Irradiations were performed with a high-pressure Mercury lamp and were carried out in NMR tubes with toluene-d_8 as solvent.[32] [b] Solvent was benzene-d_6. [c] Ratios were determined by ^{1}H NMR.

Table 5. Selected ^{1}H NMR Data of Less-Stable Molecular Motors **3b**−**9b** in Toluene-d_8

less-stable forms	chemical shift (ppm): methyl group, Me_{eq}	chemical shift (ppm): H(2′) (**3b**–**6b**), H(3′) (**7b**–**9b**)	coupling constant (Hz) $J_{H(2')-H(3')}$
3b	0.84	2.28	12.1, 7.7
4b	0.98	2.33	10.6, 9.2
5b[a]	1.02	2.39	11.0, 7.0
6b	1.02	2.40	11.7, 8.4
7b	0.96	2.28	10.6, 9.2
8b	1.14	2.40	10.4, 9.7
9b	0.86	2.76	9.2, 6.6

[a] Solvent was benzene-d_6.

directly from the slope of the straight line. In addition, an Arrhenius plot gave the activation energy (*Ea*) and preexponential factor (*A*), while an Eyring plot yielded the enthalpy of activation ($\Delta H^{\ddagger}$) and entropy of activation ($\Delta S^{\ddagger}$). From these values, the Gibbs energy of activation at room temperature (20 °C, $\Delta^{\ddagger}G^{\theta}$), rate constant at room temperature (20 °C, k^{θ}), and half-life time at room temperature (20 °C, $t_{1/2}{}^{\theta}$) were calculated. The parameters of all five motors **3**−**6** and **9** obtained by ^{1}H NMR are summarized in Table 6 .[33]

Kinetic Studies of the Thermal Conversions by CD Spectroscopy. In contrast to motors **3b**−**6b** and **9b**, the thermal conversions of less-stable motors **7b** and **8b** were expected to take place at a significant rate at room temperature which was also evident from preliminary observations on the stability of **7b** and **8b**. It was therefore decided to utilize circular dichroism (CD) spectroscopy to monitor the isomerization of **7b** and **8b** accurately as the helix inversion at temperatures below room temperature can be monitored conveniently by CD. Applying CD, however, requires pure enantiomers of **7** and **8**. Enantioresolution of the stable isomer **7a** was performed by preparative HPLC (Chiralpak OT(+)). Enantioresolution of the stable isomer **8a** was accomplished by analytical HPLC (Chiralpak OD). CD spectra at 10 °C of the first-eluted enantiomers of stable isomers **7a** and **8a** are shown in Figures 12A and 13A. These samples were irradiated by a high-pressure mercury lamp through a Pyrex filter at room temperature for 5 min to provide less-stable isomers **7b** and **8b** which in turn were subjected to CD measurements at −10 °C (Figures 12B and 13B). Although thermal conversions of less-stable isomers **7b** and **8b** take place at a significant rate at room temperature, irradiation was performed at room temperature for convenience, and the measurement of the thermal decay can be started at any initial ratio of less-stable/stable isomer. Monitoring the thermal decay started immediately after irradiation. All measurements were recorded in *n*-hexane. The CD data urged us to monitor the thermal conversions of **7b** at 229 nm and **8b** at 225 nm, since differences in $\Delta\epsilon$ values at these wavelengths are largest for **7a**/**7b** and **8a**/**8b**, respectively. For both less-stable isomers **7b** and **8b**, the thermal conversions were followed at five or six constant temperatures ranging from 5 to 30 °C at regular time intervals of 5−20 s depending on the rate of isomerization.

From the CD data thermal parameters, rate constant (*k*), half-life time ($t_{1/2}$), and Gibbs energy of activation ($\Delta G^{\ddagger}$) at each specific temperature were directly obtained from the slopes of the straight lines obtained by plotting the natural log of decay of less-stable isomers **7b** and **8b** versus time. Subsequently, the activation energy (*Ea*), preexponential factor (*A*), enthalpy of activation ($\Delta H^{\ddagger}$), entropy of activation ($\Delta S^{\ddagger}$), Gibbs energy of activation at room temperature (20 °C, $\Delta^{\ddagger}G^{\theta}$), rate constant at room temperature (20 °C, k^{θ}), and half-life time at room temperature (20 °C, $t_{1/2}{}^{\theta}$) were determined, and the data are summarized in Table 6.[33]

Discussion on the Kinetic Studies. A wide variety of reaction rates for the thermal isomerizations of the new molecular motors has been established. We decided to compare the speed of the thermal conversions by the Gibbs energy of activation at room temperature (20 °C, $\Delta^{\ddagger}G^{\theta}$), rate constant at room temperature (20 °C, k^{θ}), and half-life time at room temperature (20 °C, $t_{1/2}{}^{\theta}$).[34] Moreover, the thermodynamic parameters of the isomerization processes of the new motors at room temperature are of eminent importance in view of possible future applications. Gibbs energies of activation ($\Delta^{\ddagger}G^{\theta}$) ranging from 25.31 (Table 6, entry 4) to 21.90 kcal/mol (Table 6, entry 5) were found. The introduction of methoxy substituents at the 2 and 7 positions

(33) For details, see Supporting Information.

(34) In a previous paper[17] we preferred to quantify thermal conversions by activation energy (*Ea*). However, in these series of conversions, no correlation between *Ea* and $t_{1/2}{}^{\theta}$ was found. In fact, *Ea* is only a correlation between δT and δk.

Table 6. Thermodynamic and Kinetic Parameters of Thermal Conversions of Less-Stable Motors **3b**−**9b** to Stable Motors **3a**−**9a**

entry	less-stable motors	method	stable motors	*Ea* (kcal/mol)	$\Delta H^{\ddagger}$ (kcal/mol)	$\Delta S^{\ddagger}$ (cal/K mol)	$\Delta^{\ddagger}G^{\theta}$ (kcal/mol)	k^{θ} (s^{-1})	$t_{1/2}{}^{\theta}$ (h)
1	**3b**	NMR	**3a**	24.92 ± 0.82	24.27 ± 0.82	−3.38 ± 2.50	25.26 ± 0.07	$(8.95 \pm 1.12) \times 10^{-7}$	215 ± 27
2	**4b**	NMR	**4a**	24.20 ± 0.80	23.55 ± 0.80	−5.54 ± 2.44	25.17 ± 0.07	$(1.04 \pm 0.13) \times 10^{-6}$	184 ± 22
3	**5b**	NMR	**5a**	22.76 ± 0.81	22.13 ± 0.82	−6.50 ± 2.57	24.04 ± 0.05	$(7.32 \pm 0.60) \times 10^{-6}$	26.3 ± 2.2
4	**6b**	NMR	**6a**	24.70 ± 1.04	24.06 ± 1.04	−4.26 ± 3.22	25.31 ± 0.08	$(8.26 \pm 1.20) \times 10^{-7}$	233 ± 34
5	**7b**	CD	**7a**	21.13 ± 0.53	20.55 ± 0.53	−4.59 ± 1.82	21.90 ± 0.02	$(2.89 \pm 0.09) \times 10^{-4}$	0.67 ± 0.02
6	**8b**	CD	**8a**	21.98 ± 0.74	21.39 ± 0.73	−3.90 ± 2.48	22.54 ± 0.02	$(9.59 \pm 0.31) \times 10^{-5}$	2.01 ± 0.07
7	**9b**	NMR	**9a**	22.54 ± 0.87	21.90 ± 0.84	−8.91 ± 2.65	24.52 ± 0.05	$(3.21 \pm 0.28) \times 10^{-6}$	60.1 ± 5.3

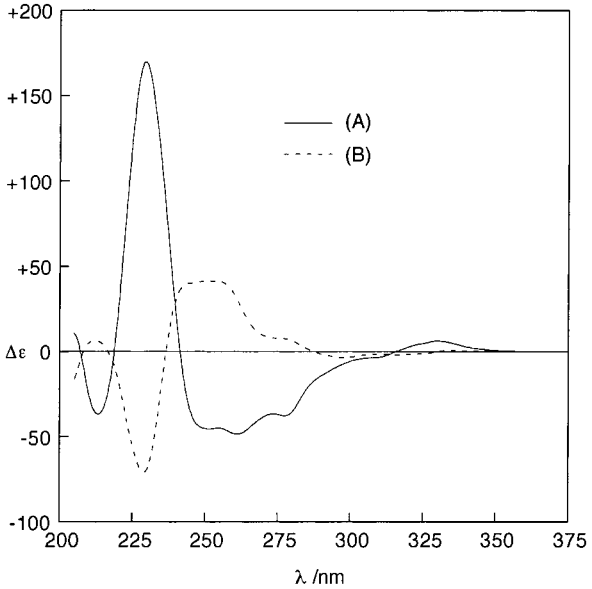

Figure 12. CD spectra of (A) the first-eluted stable enantiomer **7a** at 10 °C and (B) the irradiated sample at −10 °C (less-stable **7b**).

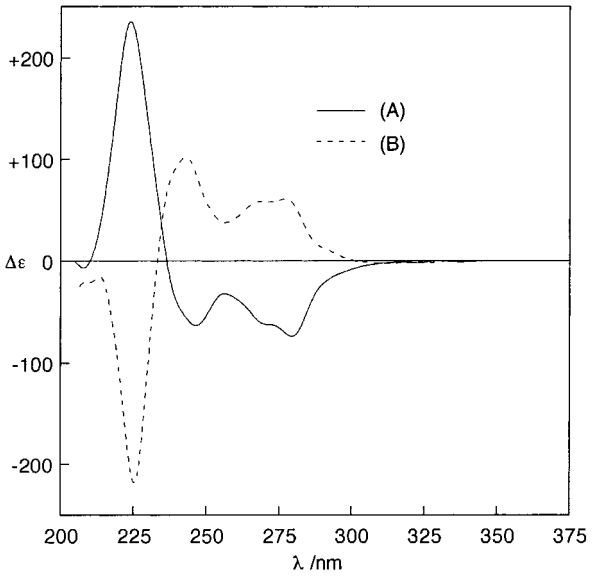

Figure 13. CD spectra of (A) the first-eluted stable enantiomer **8a** at 10 °C and (B) the irradiated sample at −10 °C (less-stable **8b**).

in the lower part has only slight influence, and surprisingly decreases the Gibbs energy of activation ($\Delta^{\ddagger}G^{\theta}$) (Table 6, entries 1 and 2). The replacement in the lower part of the large sulfur (C−S: 1.770 Å) for a smaller oxygen atom (C−O: 1.390 Å) results in a significant drop in Gibbs energy of activation ($\Delta^{\ddagger}G^{\theta}$) by 1.22 kcal/mol, and the half-life time ($t_{1/2}{}^{\theta}$) is reduced by a factor of 8 (Table 6, entries 1 and 3). When X = S, a dimethyl substituted carbon atom in the lower part (Y = CMe_2) brings along a tiny increase in Gibbs energy of activation ($\Delta^{\ddagger}G^{\theta}$) as compared with that of sulfur (Y = S) (Table 6, entries 1 and 4). As compared to motors **7** and **8**, motor **9** (Table 6, entry 7) is an exception due to its rigid and sterically demanding dibenzocycloheptene lower part (Y = CHCH) which retards thermal conversion. The most prominent decrease in Gibbs energy of activation ($\Delta^{\ddagger}G^{\theta}$) was achieved by changing the sulfur for a carbon atom in the upper part (X = CH_2) (Table 6, entries 5 and 6). The lowest Gibbs energies of activation ($\Delta^{\ddagger}G^{\theta}$) of 21.90 (Table 6, entry 5) and 22.54 kcal/mol (Table 6, entry 6) were established in these compounds. In practice, this implies that half-lives at room temperature ($t_{1/2}{}^{\theta}$) in the range 233 h (motor **6**, entry 4) to 39.9 min (motor **7**, entry 5) have been realized. The rate of the thermal step has been enhanced by approximately 3×10^3, and the isomerization time at room temperature has been reduced from hours to minutes.

Conclusions

We demonstrated repetitive unidirectional behavior performed by the second generation of light-driven molecular motors **1**−**9**. The presence of a single stereogenic center proved to be sufficient to achieve full control over the direction of rotary motion. Two energetically uphill photochemical steps and two energy relaxing thermal steps complete a four-step unidirectional 360° rotation around the central double bond as shown by motors **1** and **2** (Figure 9 and Scheme 3). No thermal cis−trans isomerization was observed. The speed of rotation of the motors was manipulated by altering the nature of atoms X and Y. A broad set, ranging from 21.90 (motor **7**) to 25.31 kcal/mol (motor **6**), of Gibbs energies of activation was ascertained. In addition, two motors, **7** and **8**, performed their photochemical conversion with stunning, near-perfect photoequilibria of 1:99.

Experimental Section

General Procedure. Melting points (uncorrected) were determined on a Mettler FP-2 melting point apparatus, equipped with a Mettler FP-21 microscope. ^{1}H NMR spectra were recorded on a Varian Gemini-200 (200 MHz), a Varian VXR-300 (300 MHz), or a Varian Unity Plus Varian-500 (500 MHz). ^{13}C NMR spectra were recorded on a Varian Gemini-200 (50 MHz), a Varian VXR-300 (75 MHz), or a Varian Unity Plus Varian-500 (125 MHz). Chemical shifts are denoted in δ-unit (ppm) relative to $CDCl_3$, and the NMR data of C_2-symmetrical compounds are listed for one-half of a molecule. The splitting patterns are designated as follows: s (singlet), d (doublet), t (triplet), q (quartet), m (multiplet), and br (broad). CD spectra were recorded on a JASCO J-715 spectropolarimeter. MS spectra were obtained with a JEOL JMS-600 spectrometer by the electron ionization (EI) procedure. Column chromatography was performed on silica gel (Aldrich 60, 230−400 mesh). The solvents were distilled and dried, if necessary, by standard methods. Reagents and starting materials were used as obtained from

Aldrich, Acros Chimica, Fluka, or Merck. Experimental procedures for compunds **11**, **12**, **13**, **18**, **20**, **25**, and **28** are given in the Supporting Information.

General Procedure for the Synthesis of Thiiranes (Episulfides) with 2,3-Dihydro-2-methyl-1*H*-naphtho[2,1-*b*]thiopyran-1-one Hydrazone 13. Under a nitrogen atmosphere, a solution of 2,3-dihydro-2-methyl-1*H*-naphtho[2,1-*b*]thiopyran-1-one hydrazone **13** (200 mg, 0.83 mmol) in dry dichloromethane (10 mL) was cooled to 0 °C, whereupon $MgSO_4$ (approximately 300 mg), Ag_2O (400 mg, 1.73 mmol), and a saturated solution of KOH in methanol (0.5 mL) were added subsequently. The mixture was stirred for 5 min at 0 °C when the color of the mixture turned red. After stirring for 30 min at 0 °C, the deep red suspension was filtrated into another ice-cooled bulb, and the remaining residue was washed with cold dichloromethane. To the deep red solution was added a solution of the appropriate thioketone in dichloromethane. Nitrogen evolution was observed, and the red color of the solution slowly disappeared. The reaction mixture was stirred overnight, and the reaction temperature was allowed to raise to room temperature. The solvents were evaporated under reduced pressure to give a residue ready for further purification.

***trans*- and *cis*-Dispiro[2,3-dihydro-2-methyl-1*H*-naphtho[2,1-*b*]thiopyran-1,2′-thiirane-3′,9″-(2″-methoxy-9″*H*-thioxanthene)] (*trans*-15 and *cis*-16).** Starting from hydrazone **13** (222 mg, 0.92 mmol) and 2-methoxy-9*H*-thioxanthene-9-thione **14** (238 mg, 0.92 mmol), the crude product was obtained following the general procedure. The unreacted thioketone was removed by column chromatography (silica gel; hexane:toluene = 10:1). The crude mixture was further purified by column chromatography (silica gel; hexane:EtOAc = 50:1) to obtain a mixture of *trans*- and *cis*-episulfide (**15** and **16**) (259 mg, 0.55 mmol, 60%). The separation of *trans*-**15** and *cis*-**16** could not be accomplished. Therefore, the mixture of *trans*-**15** and *cis*-**16** was subjected to the next step.

Dispiro[2,3-dihydro-2-methyl-1*H*-naphtho[2,1-*b*]thiopyran-1,2′-thiirane-3′,9″-(9″*H*-thioxanthene)] (29). Starting from hydrazone **13** (222 mg, 0.92 mmol) and 9*H*-thioxanthene-9-thione **24** (238 mg, 0.92 mmol), thiirane **29** was obtained as a white solid after column chromatography (silica gel; hexane:toluene = 10:1, and subsequently silica gel; hexane:EtOAc = 50:1). After crystallization from *n*-hexane, thiirane was obtained as colorless crystals (230 mg, 0.52 mmol, 60%): mp 200.4−200.5 °C. ^{1}H NMR (500 MHz, $CDCl_3$): δ 8.88 (br d, J = 8.8 Hz, 1H), 8.03−7.99 (m, 1H), 7.56 (br d, J = 8.1 Hz, 1H), 7.48 (ddd, J = 8.8, 7.0, 1.5 Hz, 1H), 7.45−7.41 (m, 1H), 7.33 (ddd, J = 8.1, 6.6, 1.1 Hz, 1H), 7.31−7.26 (m, 4H), 7.03 (dd, J = 7.7, 1.1 Hz, 1H), 6.95 (d, J = 8.4 Hz, 1H), 6.82 (dd, J = 8.1, 1.5 Hz, 1H), 6.72 (dt, J = 1.5, 7.7 Hz, 1H), 6.24 (ddd, J = 8.1, 7.0, 1.1 Hz, 1H), 2.64 (dd, J = 12.1, 7.7 Hz, 1H), 2.52 (ddq, J = 7.7, 5.5, 7.0 Hz, 1H), 2.23 (dd, J = 12.1, 5.5 Hz, 1H), 1.19 (d, J = 7.0 Hz, 3H). ^{13}C NMR (125 MHz, $CDCl_3$): δ 139.07, 136.35, 134.72, 133.66, 131.98, 131.45, 131.24, 131.20, 129.63, 128.10, 127.38, 126.93, 126.53, 126.31, 126.29, 125.61, 125.43, 125.16, 125.03, 124.53, 124.01, 123.31, 64.96, 62.01, 40.24, 34.53, 20.51. HRMS calcd for $C_{27}H_{20}S_3$: 440.0727. Found: 440.0726. Experimental procedures for the synthesis of episulfides **30**, **31**, **32** and spectroscopic data are shown in the Supporting Information.

General Procedure for the Synthesis of Thiiranes (Episulfides) with 2,3-Dihydro-3-methyl-4(1*H*)-phenanthrenone Hydrazone 18. Under a nitrogen atmosphere, a solution of 2,3-dihydro-3-methyl-4(1*H*)-phenanthrenone hydrazone **18** (300 mg, 1.34 mmol) in dry dichloromethane (15 mL) was cooled to −10 °C, whereupon $MgSO_4$ (approximately 850 mg), Ag_2O (1.20 g, 5.20 mmol), and a saturated solution of KOH in methanol (3 mL) were added successively. After stirring the mixture for 30 min at −5 °C, a red solution of diazo compound was obtained. When only an orange color was observed, more Ag_2O and KOH in methanol were added, and/or the temperature was allowed to raise to 0 °C. The purple solution was filtrated into another ice-cooled bulb, and the appropriate thioketone was added. Nitrogen evolution was observed, and thioketone was added until nitrogen formation stopped and the red color had disappeared. Stirring was continued overnight at room temperature, and the reaction temperature was allowed to raise to room temperature. The reaction mixture was concentrated under reduced pressure to give a residue which was further purified by column chromatography.

Dispiro[2,3-dihydro-3-methyl-4(1*H*)-phenanthrene-4,2′-thiirane-3′,9″-(9″*H*-thioxanthene)] (33). Starting from hydrazone **18** (370 mg, 1.66 mmol) and 9*H*-thioxanthene-9-thione **24** (200 mg, 0.88 mol), thiirane **33** was obtained as a white solid (162 mg, 0.38 mmol, 23%) after column chromatography (silica gel; hexane:EtOAc = 50:1). ^{1}H NMR (300 MHz, $CDCl_3$): δ 9.28 (d, J = 8.8 Hz, 1H), 7.98−7.95 (m, 1H), 7.53 (br d, J = 8.1 Hz, 1H), 7.45−7.39 (m, 2H), 7.34 (d, J = 8.1 Hz, 1H), 7.31−7.26 (m, 3H), 7.20 (dd, J = 8.1, 1.1 Hz, 1H), 6.95 (dd, J = 7.7, 1.1 Hz, 1H), 6.94 (d, J = 8.1 Hz, 1H), 6.66 (dt, J = 1.5, 7.7 Hz, 1H), 6.31 (ddd, J = 8.1, 7.0, 1.1 Hz, 1H), 3.56 (ddd, J = 16.5, 8.4, 7.7 Hz, 1H), 2.55 (ddd, J = 16.5, 6.6, 4.8 Hz, 1H), 2.04−1.92 (m, 1H), 1.82−1.70 (m, 1H), 1.07 (d, J = 7.0 Hz, 3H), 1.07−0.98 (m, 1H). ^{13}C NMR (75 MHz, $CDCl_3$): δ 140.93, 135.57, 134.18, 133.21, 133.10, 132.42, 132.30, 131.46, 130.36, 127.98, 127.90, 127.27, 127.19, 126.51, 126.35, 125.94, 125.86, 125.31, 124.79, 124.49, 123.90, 123.82, 66.51, 62.14, 37.51, 28.81, 28.66, 22.18. HRMS calcd for $C_{28}H_{22}S_2$: 422.1163. Found: 422.1148. Experimental procedures for the synthesis of episulfides **34**, **35** and spectroscopic data are shown in the Supporting Information.

General Procedure for the Synthesis of Olefins. Under a nitrogen atmosphere, Cu-bronze (10 equiv) was added to a stirred solution of thiirane (1 equiv) in *p*-xylene. After heating at reflux overnight, the reaction mixture was allowed to cool to room temperature. The brown copper residue was removed by silica gel filtration and washed with dichloromethane, and the solvents were evaporated under reduced pressure to give a crude product ready for further purification.

***trans*- and *cis*-2-Methoxy-9-(2′,3′-dihydro-2′-methyl$_{axial}$-1′*H*-naphtho[2,1-*b*]thiopyran-1′-ylidene)-9*H*-thioxanthene (*trans*-1a and *cis*-2a).** Starting from a mixture of *trans*- and *cis*-episulfide (*trans*-**15** and *cis*-**16**) (259 mg, 0.55 mmol), a mixture of *trans*- and *cis*-olefin (*trans*-**1a** and *cis*-**2a**) was obtained as solids. These isomers could be separated by HPLC on silica gel (hexane:EtOAc = 50:1) to give *trans*-**1a** (115 mg, 0.26 mmol, 47%) and *cis*-**2a** (107 mg, 0.24 mmol, 44%). *trans*-**1a**, ^{1}H NMR (300 MHz, $CDCl_3$): δ 7.57 (d, J = 8.4 Hz, 1H), 7.55−7.48 (m, 3H), 7.35 (d, J = 8.4 Hz, 1H), 7.25 (d, J = 6.6 Hz, 1H), 7.15 (d, J = 2.6 Hz, 1H), 7.09 (ddd, J = 8.1, 6.6, 1.4 Hz, 1H), 6.97 (ddd, J = 8.1, 7.1, 1.1 Hz, 1H), 6.84 (dd, J = 8.8, 2.6 Hz, 1H), 6.73−6.67 (m, 1H), 6.41−6.34 (m, 2H), 4.17 (ddq, J = 7.3, 2.9, 7.0 Hz, 1H), 3.86 (s, 3H), 3.69 (dd, J = 11.4, 7.3 Hz, 1H), 3.08 (dd, J = 11.4, 2.9 Hz, 1H), 0.78 (d, J = 7.0 Hz, 1H). ^{13}C NMR (75 MHz, $CDCl_3$): δ 158.35, 138.26, 137.58, 136.51, 134.89, 134.85, 132.66, 131.37, 131.27, 130.72, 128.94, 128.57, 127.48, 127.45, 127.30, 126.40, 125.99, 125.77, 125.43, 125.20, 124.39, 124.33, 113.84, 112.24, 55.56, 37.09, 32.27, 19.17. HRMS calcd for $C_{28}H_{22}OS_2$: 438.1112. Found: 438.1095. *cis*-**2a**, ^{1}H NMR (300 MHz, $CDCl_3$): δ 7.62−7.52 (m, 5H), 7.37 (d, J = 8.8 Hz, 1H), 7.33 (dt, J = 1.5, 7.7 Hz, 1H), 7.25 (dt, J = 1.5, 7.7 Hz, 1H), 7.12 (d, J = 8.8 Hz, 1H), 7.11 (br t, J = 7.0 Hz, 1H), 7.00 (br t, J = 7.0 Hz, 1H), 6.30 (dd, J = 8.4, 2.6 Hz, 1H), 5.92 (d, J = 2.6 Hz, 1H), 4.11 (ddq, J = 7.3, 3.3, 7.0 Hz, 1H), 3.69 (dd, J = 11.5, 7.3 Hz, 1H), 3.06 (dd, J = 11.5, 3.3 Hz, 1H), 3.01 (s, 3H), 0.79 (d, J = 7.0 Hz, 3H). ^{13}C NMR (75 MHz, $CDCl_3$): δ 157.60, 139.39, 136.66, 136.46, 135.87, 134.89, 132.60, 131.51, 131.41, 130.90, 127.68, 127.53, 127.45, 127.38, 127.16, 126.67, 125.98, 125.93, 125.43, 125.36, 124.49, 124.33, 114.39, 112.91, 54.81, 37.17, 32.27, 19.24. HRMS calcd for $C_{28}H_{22}OS_2$: 438.1112. Found: 438.1099. Enantioresolution of *trans*-**1a** was accomplished by preparative chiral HPLC (Chiralpak OD, heptane:2-propanol = 99:1). The second-eluted enantiomer was crystallized from *n*-hexane to give colorless prisms (mp 214.9 °C) of [CD(−)277.2]-*trans*-**1a** suitable for X-ray crystallographic analysis. Enantioresolution of *cis*-**2a** was achieved by preparative chiral HPLC (Chiralpak OD, heptane:2-propanol = 99:1).

9-(2′,3′-Dihydro-2′-methyl$_{axial}$-1′*H*-naphtho[2,1-*b*]thiopyran-1′-ylidene)-9*H*-thioxanthene (3a). Starting from episulfide **29** (120 mg, 0.27 mmol), olefin **3a** was obtained and purified by recrystallization from *n*-hexane to yield colorless prisms (106 mg, 0.26 mmol, 95%): mp 220.4−220.6 °C. ^{1}H NMR (500 MHz, $CDCl_3$): δ 7.64−7.58 (m, 3H), 7.56−7.54 (m, 2H), 7.38 (d, J = 8.4 Hz, 1H), 7.36 (dt, J = 1.1, 7.3 Hz, 1H), 7.30−7.26 (m, 2H), 7.11 (ddd, J = 8.1, 7.0, 1.1 Hz, 1H), 6.99 (ddd, J = 8.4, 7.0, 1.5 Hz, 1H), 6.73 (ddd, J = 7.7, 6.6, 2.2 Hz, 1H), 6.43−6.38 (m, 2H), 4.13 (ddq, J = 7.3, 2.9, 6.6 Hz, 1H), 3.72 (dd, J = 11.4, 7.3 Hz, 1H), 3.09 (dd, J = 11.4, 2.9 Hz, 1H), 0.78 (d, J = 6.6 Hz, 3H). ^{13}C NMR (125 MHz, $CDCl_3$): δ 138.24, 136.43, 136.08, 136.05, 134.90, 134.19, 132.44, 131.34, 131.22, 130.70, 128.97, 127.71, 127.56, 127.49, 126.70, 126.38, 126.12, 126.03, 125.75, 125.42, 125.31, 124.34, 124.30, 37.18, 32.12, 19.19. HRMS calcd for $C_{27}H_{20}S_2$: 408.1006. Found: 408.1016.

2,7-Dimethoxy-9-(2′,3′-dihydro-2′-methyl$_{axial}$-1′*H*-naphtho[2,1-*b*]-thiopyran-1′-ylidene)-9*H*-thioxanthene (4a). Starting from episulfide **30** (200 mg, 0.40 mmol), olefin **4a** was obtained, after purification by recrystallization from *n*-hexane, as colorless prisms (185 mg, 0.40 mmol, 99%): mp 149.0−149.2 °C. ^{1}H NMR (500 MHz, $CDCl_3$): δ 7.60 (d, J = 8.8 Hz, 1H), 7.56 (br d, J = 7.3 Hz, 1H), 7.51 (d, J = 8.8 Hz, 1H), 7.38 (d, J = 8.4 Hz, 1H), 7.17 (d, J = 2.6 Hz, 1H), 7.14 (m, 1H), 7.12 (d, J = 8.8 Hz, 1H), 7.01 (br t, J = 7.7 Hz, 1H), 6.85 (dd, J = 8.8, 2.9 Hz, 1H), 6.30 (dd, J = 8.4, 2.6 Hz, 1H), 5.93 (d, J = 2.9 Hz, 1H), 4.20 (ddq, J = 7.7, 3.3, 6.6 Hz, 1H), 3.88 (s, 3H), 3.71 (dd, J = 11.4, 7.7 Hz, 1H), 3.08 (dd, J = 11.4, 3.3 Hz, 1H), 3.03 (s, 3H), 0.82 (d, J = 6.6 Hz, 3H). ^{13}C NMR (75 MHz, $CDCl_3$): δ 158.27, 157.55, 139.43, 137.44, 136.56, 134.88, 132.82, 131.54, 131.46, 130.93, 128.57, 127.93, 127.47, 127.43, 127.22, 126.14, 125.98, 125.39, 124.54, 124.42, 114.39, 113.89, 112.95, 112.22, 55.59, 54.88, 37.15, 32.44, 19.33. HRMS calcd for $C_{29}H_{24}O_2S_2$: 468.1218. Found: 468.1217.

9-(2′,3′-Dihydro-2′-methyl$_{axial}$-1′*H*-naphtho[2,1-*b*]thiopyran-1′-ylidene)-9*H*-xanthene (5a). Starting from episulfide **31** (70 mg, 0.17 mmol), olefin **5a** was obtained, after purification by recrystallization from EtOAc, as slightly yellow prisms (63 mg, 0.16 mmol, 97%): mp 238.8−239.0 °C. ^{1}H NMR (500 MHz, $CDCl_3$): δ 7.63 (d, J = 8.4 Hz, 1H), 7.60 (br d, J = 8.1 Hz, 1H), 7.59 (dd, J = 7.7, 1.1 Hz, 1H), 7.38 (d, J = 8.4 Hz, 1H), 7.37 (ddd, J = 8.4, 7.0, 1.5 Hz, 1H), 7.33 (dt, J = 1.5, 7.7 Hz, 1H), 7.29 (br d, J = 8.4 Hz, 1H), 7.23 (dt, J = 1.5, 7.7 Hz, 1H), 7.12 (ddd, J = 8.1, 7.0, 1.1 Hz, 1H), 7.06 (d, J = 8.1 Hz, 1H), 6.96 (ddd, J = 8.4, 7.0, 1.5 Hz, 1H), 6.85−6.81 (m, 1H), 6.23−6.20 (m, 2H), 4.29 (ddq, J = 7.0, 2.6, 6.6 Hz, 1H), 3.77 (dd, J = 11.0, 7.0 Hz, 1H), 3.21 (dd, J = 11.0, 2.6 Hz, 1H), 0.79 (d, J = 6.6 Hz, 3H). ^{13}C NMR (125 MHz, $CDCl_3$): δ 154.87, 153.43, 134.78, 134.55, 131.40, 130.83, 130.28, 128.26, 128.19, 127.70, 127.61, 127.45, 126.76, 126.16, 125.81, 125.39, 125.08, 124.29, 123.95, 123.38, 123.01, 122.19, 116.90, 115.89, 37.03, 30.75, 18.48. HRMS calcd for $C_{27}H_{20}OS$: 392.1235. Found: 392.1224.

10,10-Dimethyl-9-(2′,3′-dihydro-2′-methyl$_{axial}$-1′*H*-naphtho[2,1-*b*]-thiopyran-1′-ylidene)-10*H*-anthracene (6a). Starting from episulfide **32** (160 mg, 0.36 mmol), olefin **6a** was obtained, after purification by recrystallization from *n*-hexane, as colorless prisms (125 mg, 0.30 mmol, 85%): mp 202.3−202.7 °C. ^{1}H NMR (300 MHz, $CDCl_3$): δ 7.71−7.58 (m, 4H), 7.51−7.49 (m, 1H), 7.48 (d, J = 8.4 Hz, 1H), 7.36−7.24 (m, 3H), 7.14 (br t, J = 7.3 Hz, 1H), 6.93 (br t, J = 7.3 Hz, 1H), 6.79 (ddd, J = 8.1, 7.0, 1.1 Hz, 1H), 6.26 (br t, J = 7.3 Hz, 1H), 6.15 (br d, J = 7.3 Hz, 1H), 4.41 (ddq, J = 8.8, 3.3, 7.0 Hz, 1H), 3.69 (dd, J = 11.7, 8.8 Hz, 1H), 3.00 (dd, J = 11.7, 3.3 Hz, 1H), 0.82 (d, J = 7.0 Hz, 3H). ^{13}C NMR (75 MHz, $CDCl_3$): δ 147.57, 144.43, 137.79, 137.39, 135.19, 134.81, 134.10, 132.37, 131.90, 127.84, 127.68, 127.40, 126.96, 126.74, 126.07, 125.30, 125.12, 125.07, 124.45, 124.37, 123.45, 122.97, 40.18, 37.17, 34.47, 31.78, 25.22, 20.40. HRMS calcd for $C_{30}H_{26}S$: 418.1755. Found: 418.1740.

9-[2′,3′-Dihydro-3′-methyl$_{axial}$-4′(1′*H*)-phenanthrenylidene]-9*H*-thioxanthene (7a). Starting from episulfide **33** (100 mg, 0.24 mmol), olefin **7a** was obtained as a white solid (77 mg, 0.20 mmol, 83%) after column chromatography (hexane:EtOAc = 50:1). Recrystallization from *n*-hexane yielded colorless prisms: mp 210.9−211.2 °C. ^{1}H NMR (500 MHz, $CDCl_3$): δ 7.66 (d, J = 8.1 Hz, 1H), 7.62−7.22 (m, 3H), 7.48 (d, J = 8.4 Hz, 1H), 7.35−7.31 (m, 3H), 7.26−7.22 (m, 1H), 7.11 (t, J = 7.5 Hz, 1H), 6.95 (dt, J = 1.4, 7.5 Hz, 1H), 6.72 (dt, J = 1.4, 7.5 Hz, 1H), 6.24 (d, J = 7.5 Hz, 1H), 3.90 (ddq, J = 8.4, 4.0, 7.0 Hz, 1H), 3.04 (ddd, J = 15.0, 10.3, 7.7 Hz, 1H), 2.95 (ddd, J = 15.0, 6.2, 2.7 Hz, 1H), 2.57 (dddd, J = 12.9, 8.4, 7.7, 2.7 Hz, 1H), 1.47 (dddd, J = 12.9, 10.3, 6.2, 4.0 Hz, 1H), 0.82 (d, J = 7.0 Hz, 3H). ^{13}C NMR (75 MHz, $CDCl_3$): δ 138.82, 138.76, 138.58, 136.67, 136.01, 134.45, 133.72, 131.93, 131.52, 129.94, 128.40, 128.35, 127.72, 127.36, 127.25, 126.60, 126.34, 126.02, 125.71, 125.54, 125.21, 125.16, 125.07, 124.14, 30.97, 30.63, 29.02, 21.72. HRMS calcd for $C_{28}H_{22}S$: 390.1442. Found: 390.1449. Enantioresolution of **7a** was achieved by preparative chiral HPLC (Chiralpak OT(+) (Ø = 4.6 mm, l = 250 mm), heptane:2-propanol = 99.95:0.05). The solvent of the first-eluted enantiomer was evaporated under reduced pressure, and the obtained product was dissolved in *n*-hexane to be analyzed by CD spectroscopy.

10,10-Dimethyl-9-[2′,3′-dihydro-3′-methyl$_{axial}$-4′(1′*H*)-phenanthrenylidene]-10*H*-anthracene (8a). Starting from episulfide **34** (80 mg, 0.19 mmol), olefin **8a** was obtained, after purification by recrystallization from *n*-hexane, as colorless prisms (50 mg, 0.12 mmol, 63%): mp 189.0−189.3 °C. ^{1}H NMR (500 MHz, $CDCl_3$): δ 7.72 (d, J = 8.4 Hz, 1H), 7.68 (d, J = 8.8 Hz, 1H), 7.64−7.62 (m, 1H), 7.58−7.56 (m, 1H), 7.46 (d, J = 8.4 Hz, 1H), 7.41 (d, J = 8.4 Hz, 1H), 7.37 (d, J = 8.1 Hz, 1H), 7.30−7.25 (m, 2H), 7.16 (t, J = 7.7 Hz, 1H), 6.92 (t, J = 7.7 Hz, 1H), 6.81 (t, J = 7.3 Hz, 1H), 6.27 (t, J = 7.7 Hz, 1H), 6.18 (d, J = 7.3 Hz, 1H), 4.10 (ddq, J = 9.3, 2.8, 6.6 Hz, 1H), 3.00 (ddd, J = 14.3, 11.7, 7.5 Hz, 1H), 2.93 (ddd, J = 14.3, 6.6, 1.8 Hz, 1H), 2.65 (dddd, J = 12.8, 9.3, 6.6, 1.8 Hz, 1H), 1.92 (s, 3H), 1.85 (s, 3H), 1.46 (dddd, J = 12.8, 11.7, 6.6, 3.3 Hz, 1H), 0.65 (d, J = 6.6 Hz, 3H). ^{13}C NMR (50 MHz, $CDCl_3$): δ 147.42, 144.65, 138.59, 138.37, 137.81, 136.80, 135.32, 132.23, 131.44, 130.52, 128.36, 127.64, 127.18, 126.93, 126.57, 126.02, 125.80, 125.74, 125.11, 124.54, 124.38, 124.13, 123.25, 122.91, 40.20, 31.92, 31.10, 30.84, 29.50, 24.94, 22.26. HRMS calcd for $C_{31}H_{28}$: 400.2191. Found: 400.2189. Enantioresolution of **8a** was achieved by preparative chiral HPLC (Chiralpak OD (Ø = 2.0 mm, l = 100 mm), heptane:2-propanol = 99.9:0.1). The solvent of the first-eluted enantiomer was evaporated under reduced pressure, and the obtained product was dissolved in *n*-hexane to be analyzed by CD spectroscopy.

5-[2′,3′-Dihydro-3′-methyl$_{axial}$-4′(1′*H*)-phenanthrenylidene]-5*H*-dibenzo[*a*,*d*]cycloheptene (9a). Under a nitrogen atmosphere, thiirane **35** (40 mg, 0.096 mmol) and triphenylphosphine (51 mg, 0.19 mmol) were dissolved in toluene (7 mL). This mixture was refluxed for 44 h. After cooling, the solvent was evaporated under reduced pressure, and the residue was purified by column chromatography (silica gel, hexane:dichloromethane = 15:1). The obtained solid was recrystallized twice from Et_2O, to remove triphenylphosphine, to provide pure olefin **9a** as colorless crystals (20 mg, 0.052 mmol, 54%): mp 192.2−192.6 °C. ^{1}H NMR (500 MHz, $CDCl_3$): δ 7.59 (d, J = 8.4 Hz, 1H), 7.55 (d, J = 8.1 Hz, 1H), 7.51 (d, J = 8.4 Hz, 1H), 7.42−7.38 (m, 3H), 7.31−7.28 (m, 2H), 7.15−7.08 (m, 4H), 6.99 (t, J = 8.4 Hz, 1H), 6.74 (t, J = 7.7 Hz, 1H), 6.54 (t, J = 7.7 Hz, 1H), 6.28 (t, J = 7.7 Hz, 1H), 3.46 (ddq, J = 9.0, 5.5, 6.6 Hz, 1H), 2.97 (ddd, J = 14.3, 12.4, 6.6 Hz, 1H), 2.86 (ddd, J = 14.3, 5.3, 2.4 Hz, 1H), 2.45 (dddd, J = 12.8, 9.0, 6.6, 2.4 Hz, 1H), 1.46 (dddd, J = 12.8, 12.4, 5.5, 5.3 Hz, 1H), 0.57 (d, J = 6.6 Hz, 3H). ^{13}C NMR (50 MHz, $CDCl_3$): δ 141.47, 139.19, 138.99, 138.99, 138.15, 136.12, 135.50, 134.39, 133.85, 131.77, 131.52, 130.17, 128.91, 128.31, 128.06, 128.02, 127.81, 127.22, 127.17, 126.68, 126.37, 125.84, 125.71, 125.17, 124.42, 124.01, 31.15, 31.01, 29.75, 21.92. HRMS calcd for $C_{30}H_{24}$: 384.1878. Found: 384.1863.

General Procedure of Irradiation Experiments. Irradiations were carried out with a 180 W high-pressure mercury lamp using an appropriate filter. The samples in an NMR tube or quartz cell were directly analyzed by ^{1}H NMR or CD measurements, respectively.

***trans*-2-Methoxy-9-(2′,3′-dihydro-2′-methyl$_{equatorial}$-1′*H*-naphtho-[2,1-*b*]thiopyran-1′-ylidene)-9*H*-thioxanthene (*trans*-1b).** Twenty-five milligrams (5.70×10^{-2} mmol) of *cis*-olefin **2a** was dissolved in 3 mL of hexane−dichloromethane (10:1). This solution in a quartz cell was irradiated by a Hg-lamp using a 365 nm filter at 10 °C for 12 h. After evaporation of solvents under reduced pressure, less-stable *trans*-olefin **1b** was obtained. ^{1}H NMR showed an 11:89 ratio of starting material (*cis*-**2a**):product (*trans*-**1b**). Less-stable *trans*-**1b**, ^{1}H NMR (300 MHz, $CDCl_3$): δ 7.60 (d, J = 8.7 Hz), 7.57 (d, J = 8.2 Hz, 1H), 7.50 (d, J = 8.7 Hz, 1H), 7.44 (d, J = 8.7 Hz, 1H), 7.41 (d, J = 8.7 Hz, 1H), 7.31 (d, J = 7.7 Hz, 1H), 7.19 (d, J = 2.6 Hz, 1H), 7.13 (br t, J = 7.7 Hz, 1H), 6.99 (br t, J = 7.7 Hz, 1H), 6.85 (dd, J = 8.7, 2.6 Hz, 1H), 6.71 (ddd, J = 7.7, 6.9, 1.1 Hz, 1H), 6.42−6.36 (m, 2H), 3.85 (s, 3H), 3.52 (dd, J = 9.9, 7.3 Hz, 1H), 3.32 (dd, J = 12.1, 9.9 Hz, 1H), 2.74 (ddq, J = 12.1, 7.3, 7.0 Hz, 1H), 1.17 (d, J = 7.0 Hz, 3H).

***cis*-2-Methoxy-9-(2′,3′-dihydro-2′-methyl$_{equatorial}$-1′*H*-naphtho[2,1-*b*]thiopyran-1′-ylidene)-9*H*-thioxanthene (*cis*-2b).** Twenty-five milligrams (5.70×10^{-2} mmol) of *trans*-olefin **1a** was dissolved in 3 mL of hexane−dichloromethane (10:1). This solution in a quartz cell was irradiated by a Hg-lamp using a 365 nm filter at 10 °C for 12 h. After evaporation of solvents under reduced pressure, less-stable *cis*-olefin **2b** was obtained. ^{1}H NMR showed a 14:86 ratio of starting material (*trans*-**1a**):product (*cis*-**2b**). ^{1}H NMR (300 MHz, $CDCl_3$): δ 7.63−7.58 (m, 4H), 7.45 (br d, J = 8.4 Hz, 1H), 7.42 (d, J = 8.4 Hz, 1H), 7.32−7.26 (m, 2H), 7.19 (d, J = 8.4 Hz, 1H), 7.16 (br t, J = 7.7 Hz, 1H), 7.02 (br t, J = 7.7 Hz, 1H), 6.31 (dd, J = 8.4, 2.6 Hz, 1H), 5.94 (d, J = 2.6 Hz, 1H), 3.51 (dd, J = 10.1, 7.3 Hz, 1H), 3.33 (dd, J = 12.4, 10.1 Hz, 1H), 2.99 (s, 3H), 2.76 (ddq, J = 12.4, 7.3, 7.0 Hz, 1H), 1.10 (d, J = 7.0 Hz, 1H).

9-(2′,3′-Dihydro-2′-methyl$_{equatorial}$-1′*H*-naphtho[2,1-*b*]thiopyran-1′-ylidene)-9*H*-thioxanthene (3b). Eighteen milligrams (4.41×10^{-2} mmol) of olefin **3a** was dissolved in 0.6 mL of toluene-d_8. This solution was irradiated by a Hg-lamp using a Pyrex filter for 3 h at room temperature. ^{1}H NMR revealed an 8:92 ratio of **3a**:**3b**. ^{1}H NMR (300 MHz, toluene-d_8): δ 7.71−7.68 (m, 1H), 7.43−7.34 (m, 5H), 7.19 (br d, J = 7.7 Hz, 1H), 7.00−6.87 (m, 4H), 6.55 (br d, J = 8.4 Hz, 1H), 6.39 (dt, J = 1.1, 7.7 Hz, 1H), 6.16 (dt, J = 1.1, 7.7 Hz, 1H), 3.02 (dd, J = 9.9, 7.7 Hz, 1H), 2.92 (dd, J = 12.1, 9.9 Hz, 1H), 2.28 (ddq, J = 12.1, 7.7, 7.0 Hz, 1H), 0.84 (d, J = 7.0 Hz, 3H).

2,7-Dimethoxy-9-(2′,3′-dihydro-2′-methyl$_{equatorial}$-1′*H*-naphtho[2,1-*b*]thiopyran-1′-ylidene)-9*H*-thioxanthene (4b). Twenty milligrams (4.27×10^{-2} mmol) of olefin **4a** was dissolved in 0.6 mL of toluene-d_8. This solution was irradiated by a Hg-lamp using a Pyrex filter for 3 h at room temperature. ^{1}H NMR revealed a 13:87 ratio of **4a**:**4b**. ^{1}H NMR (300 MHz, toluene-d_8): δ 7.77 (d, J = 8.1 Hz, 1H), 7.39−7.30 (m, 3H), 7.17 (d, J = 2.6 Hz, 1H), 7.12 (d, J = 8.4 Hz, 1H), 7.07−6.91 (m, 3H), 6.51 (dd, J = 8.4, 2.6 Hz, 1H), 6.21 (dd, J = 8.4, 2.9 Hz, 1H), 6.15 (d, J = 2.9 Hz, 1H), 3.31 (s, 3H), 3.07−2.96 (m, 2H), 2.73 (s, 3H), 2.33 (ddq, J = 10.6, 9.2, 7.0 Hz, 1H), 0.98 (d, J = 7.0 Hz, 3H).

9-(2′,3′-Dihydro-2′-methyl$_{equatorial}$-1′*H*-naphtho[2,1-*b*]thiopyran-1′-ylidene)-9*H*-xanthene (5b). Twelve milligrams (3.06×10^{-2} mmol) of olefin **5a** was dissolved in 0.6 mL of benzene-d_6. This solution was irradiated by a Hg-lamp using a 365 nm filter for 24 h at room temperature. ^{1}H NMR revealed a 23:77 ratio of **5a**:**5b**. ^{1}H NMR (300 MHz, benzene-d_6): δ 7.51−7.46 (m, 2H), 7.43−7.27 (m, 3H), 7.23 (dd, J = 8.1, 1.1 Hz, 1H), 7.10−6.82 (m, 5H), 6.53 (ddd, J = 8.8, 7.3, 1.5 Hz, 1H), 6.43 (dd, J = 7.7, 1.5 Hz, 1H), 6.03 (ddd, J = 8.8, 7.7, 1.1 Hz, 1H), 2.98 (dd, J = 11.0, 9.9 Hz, 1H), 2.95 (dd, J = 9.9, 7.0 Hz, 1H), 2.39 (ddq, J = 11.0, 7.0, 7.0 Hz, 1H), 1.02 (d, J = 7.0 Hz, 3H).

10,10-Dimethyl-9-(2′,3′-dihydro-2′-methyl$_{equatorial}$-1′*H*-naphtho-[2,1-*b*]thiopyran-1′-ylidene)-10*H*-anthracene (6b). Fifteen milligrams (3.58×10^{-2} mmol) of olefin **6a** was dissolved in 0.6 mL of toluene-d_8. This solution was irradiated by a Hg-lamp using a Pyrex filter for 2 h at room temperature. ^{1}H NMR revealed an 8:92 ratio of **6a**:**6b**. ^{1}H NMR (300 MHz, toluene-d_6): δ 7.56−7.41 (m, 4H), 7.31 (dd, J = 7.7, 1.1 Hz, 1H), 7.18−7.08 (m, 3H), 7.06−6.97 (m, 2H), 6.87 (ddd, J = 8.4, 7.0, 1.1 Hz, 1H), 6.62 (dt, J = 1.5, 7.7 Hz, 1H), 6.39 (dd, J = 7.7, 1.5 Hz, 1H), 6.14 (dt, J = 1.1, 7.7 Hz, 1H), 3.12 (dd, J = 10.3, 8.4 Hz, 1H), 2.98 (dd, J = 11.7, 10.3 Hz, 1H), 2.40 (ddq, J = 11.7, 8.4, 7.0 Hz, 1H), 1.02 (d, J = 7.0 Hz, 3H).

9-[2′,3′-Dihydro-3′-methyl$_{equatorial}$-4′(1′*H*)-phenanthrenylidene]-9*H*-thioxanthene (7b). Ten milligrams (2.56×10^{-2} mmol) of olefin **7a** was dissolved in 0.75 mL of toluene-d_8. This solution was irradiated by a Hg-lamp using a Pyrex filter for 17 h at −25 °C. ^{1}H NMR revealed a 1:99 ratio of **7a**:**7b**. ^{1}H NMR (500 MHz, toluene-d_8, −25 °C): δ 7.82 (d, J = 7.7 Hz, 1H), 7.55 (d, J = 8.4 Hz, 1H), 7.51 (dd, J = 7.7, 1.5 Hz, 1H), 7.41 (dd, J = 7.7, 1.1 Hz, 1H), 7.38 (dd, J = 7.7, 1.5 Hz, 1H), 7.31 (d, J = 7.7 Hz, 1H), 7.24 (d, J = 8.4 Hz, 1H), 7.07−7.01 (m, 2H), 6.96 (dt, J = 1.1, 7.3 Hz, 1H), 6.91 (dt, J = 1.5, 7.7, 1H), 6.45 (dd, J = 7.7, 1.5 Hz, 1H), 6.43 (dd, J = 7.7, 1.1 Hz, 1H), 6.16 (dt, J = 1.1, 7.7 Hz, 1H), 3.17 (ddd, J = 15.0, 10.6, 9.0 Hz, 1H), 2.77 (dd, J = 15.0, 8.4 Hz, 1H), 2.28 (ddq, J = 10.6, 9.2, 7.0 Hz, 1H), 1.92 (dddd, J = 11.8, 9.2, 9.0, 8.4 Hz, 1H), 1.75 (ddd, J = 11.8, 10.6, 10.6 Hz, 1H), 0.96 (d, J = 7.0 Hz, 3H).

10,10-Dimethyl-9-[2′,3′-dihydro-3′-methyl$_{equatorial}$-4′(1′*H*)-phenanthrenylidene]-10*H*-anthracene (8b). Olefin **8a** (9.8 mg, 2.45×10^{-2} mmol) was dissolved in 0.75 mL of toluene-d_8. This solution was irradiated by a Hg-lamp using a Pyrex filter for 17 h at −25 °C. ^{1}H NMR revealed a 1:99 ratio of **8a**:**8b**. ^{1}H NMR (500 MHz, toluene-d_8, −25 °C): δ 7.68−7.61 (m, 3H), 7.52 (dd, J = 7.3, 1.1 Hz, 1H), 7.32−7.30 (m, 2H), 7.21 (d, J = 8.1 Hz, 1H), 7.17−7.05 (m, 3H), 6.99 (t, J = 8.1 Hz, 1H), 6.72 (dt, J = 1.1, 7.3, 1H), 6.50 (d, J = 7.7 Hz, 1H), 6.22 (t, J = 7.3 Hz, 1H), 3.16 (ddd, J = 14.7, 10.2, 9.9 Hz, 1H), 2.77 (dd, J = 14.7, 8.1 Hz, 1H), 2.40 (ddq, J = 10.4, 9.7, 7.0 Hz, 1H), 1.97 (dddd, J = 11.8, 9.9, 9.7, 8.1 Hz, 1H), 1.92 (s, 3H), 1.88 (ddd, J = 11.8, 10.4, 10.2 Hz, 1H), 1.68 (s, 3H), 1.14 (d, J = 7.0 Hz, 3H).

5-[2′,3′-Dihydro-3′-methyl$_{equatorial}$-4′(1′*H*)-phenanthrenylidene]-5*H*-dibenzo[*a*,*d*]cycloheptene (9b). Olefin **9a** (10.4 mg, 2.71×10^{-2} mmol) was dissolved in 0.75 mL of toluene-d_6. This solution was irradiated by a Hg-lamp using a Pyrex filter for 168 h at room temperature. ^{1}H NMR revealed a 25:75 ratio of **9a**:**9b**. ^{1}H NMR (500 MHz, toluene-d_8): δ 8.63 (d, J = 8.1 Hz, 1H), 7.62 (d, J = 7.7 Hz, 1H), 7.55 (d, J = 8.1 Hz, 1H), 7.49 (dd, J = 8.1, 0.7 Hz, 1H), 7.48 (d, J = 8.1 Hz, 1H), 7.27 (d, J = 8.1 Hz, 1H), 7.26 (dd, J = 7.7, 1.5 Hz, 1H), 7.17 (dd, J = 7.7, 0.7 Hz, 1H), 7.00 (d, J = 7.7 Hz, 1H), 6.91 (d, J = 8.1 Hz, 1H), 6.74 (d, J = 11.7 Hz, 1H), 6.71 (dd, J = 7.7, 0.7 Hz, 1H), 6.64 (d, J = 11.7 Hz, 1H), 6.62 (t, J = 7.7 Hz, 1H), 6.55 (dt, J = 0.7, 7.7 Hz, 1H), 6.53 (t, J = 7.7 Hz, 1H), 2.76 (ddq, J = 9.2, 6.6, 7.0 Hz, 1H), 2.57 (ddd, J = 13.2, 13.2, 5.7 Hz, 1H), 2.27 (ddd, J = 13.2, 4.6, 2.2 Hz, 1H), 1.76 (dddd, J = 12.7, 9.2, 5.7, 2.2 Hz, 1H), 0.66 (dddd, J = 13.2, 12.7, 6.6, 4.6 Hz, 1H), 0.61 (d, J = 7.0 Hz, 3H).

X-ray crystallography of (2′*R*)-(*M*)-*trans*-**1a**, racemic (2′*R**)-(*P**)-*trans*-**1b**, **8a**, and **9a** can be found in the Supporting Information.

Kinetics Studies of Isomerization of Less-Stable Motors 3b, 4b, 5b, 6b, and 9b to Stable Motors 3a, 4a, 5a, 6a, and 9a by ^{1}H NMR. The kinetic conversions of the irradiated samples, in toluene-d_8 or benzene-d_6, were carried out at a constant temperature in the range 35−65 °C. The NMR tube containing the sample was heated in a water bath and immediately cooled to 0 °C, to stop reaction, when measured. At each temperature, ^{1}H NMR spectra were recorded at 9 or 10 regular time intervals. The ratios of less-stable form/stable form were determined by comparison of the integral values of chemical shifts of less-stable form and stable form. With these ratios, the conversions of less-stable form into stable form were calculated and analyzed applying equations for first-order reaction. The rate constants (k) of isomerization were determined, and the thermal parameters ($\Delta G^{\ddagger}$, Ea, $\Delta H^{\ddagger}$, $\Delta S^{\ddagger}$, etc.) were subsequently also determined.

Kinetics Studies of Isomerization of Less-Stable Motors 7b and 8b to Stable Motors 7a and 8a by CD Spectra. The CD spectra of

the solutions of the first-eluted enantiomers, (2′*S*)-(*M*)-**7a** and (2′*S*)-(*M*)-**8a**, in *n*-hexane (concentrations of these solutions were 2.64×10^{-5} (**7**) and 1.88×10^{-5} M (**8**), respectively) were measured at several temperatures in the range 5−30 °C. Irradiation of these solutions was performed by a high-pressure mercury lamp through a Pyrex filter for 5 min to reach the photostationary states. Using these solutions, the intensities of CD values at 229.0 nm (**7**) or 225.0 nm (**8**), respectively, were monitored at 5, 10, or 20 s intervals at a constant temperature in the range 5−30 °C for 1−5 h. The conversions of less-stable form into stable form were determined from the changes of $\Delta\epsilon$ values and analyzed applying equations of first-order reaction. The rate constants (k) of the isomerization were determined, and the thermal parameters ($\Delta G^{\ddagger}$, Ea, $\Delta H^{\ddagger}$, $\Delta S^{\ddagger}$, etc.) were subsequently also determined.

Acknowledgment. We thank N. J. Buurma for discussion on the kinetic studies. Financial support from The Netherlands Foundation for Scientific Research (NWO-CW) is gratefully acknowledged.

Supporting Information Available: Experimental procedures of all new compounds as well as their spectroscopic data, X-ray crystallography information of olefins **1a**, **1b**, **8a**, **9a**, and all kinetic data of thermal interconversion of motors **3**−**9** (PDF). This material is available free of charge via the Internet at http://pubs.acs.org.

JA012499I